RECIRCULATION IN A CONFINED TURBULENT DIFFUSION FLAME

MIHA ZUMER

Submitted to the Faculty of Graduate Studies and Research of McGill University in partial fulfillment of the requirements for the degree Master of Engineering

Thesis Supervisor: Dr. John M. Dealy

Department of Chemical Engineering
McGill University, Montreal, Canada

June, 1967

ACKNOWLEDGEMENTS

The author wishes to express his gratitude to:

Dr. J.M. Dealy for his kind assistance and guidance in all aspects of this thesis.

The National Research Council for research equipment grants and financial support.

The machinists and the technical personnel of the Chemical Engineering Department for their valuable service and advice.

Prof. R. Modic and the University of Ljubljana for their encouragement and support.

Chemical Engineering M.Eng.

RECIRCULATION IN A CONFINED TURBULENT DIFFUSION FLAME

Miha Zumer

ABSTRACT

The existence of recirculation patterns in combustion chambers can have an important effect on their performance; accordingly recirculation has been the subject of a number of studies. These studies have involved mainly the influence of recirculation on the parameters of the system; only few authors have attempted to predict the onset of recirculation, based on a cold model.

In the present study, recent results of confined incompressible jets were used as a basis to develop a dimensionless parameter which serves as an approximate criterion for the prediction of the onset of recirculation in a confined turbulent diffusion flame.

Confined jet and diffusion flame phenomena are briefly reviewed and previous work on recirculation in incompressible jets and confined jet flames is discussed. The experimental equipment and the experimental technique used are described. The onset of recirculation as indicated by temperature measurements is correlated by means of a dimensionless parameter indicated by the approximate integral momentum analysis.

TABLE OF CONTENTS

LIST OF FIGURES

INTRODUCTION

When a high velocity stream of fluid discharges into another stream it is called a jet. When one of the streams is a fuel and another is an oxidizing agent, for example air, with combustion taking place, it is called a jet flame or a diffusion flame. If the combustion occurs in a confined region such as a tube, we would refer to the configuration as a confined jet diffusion flame. A number of flames of practical interest are of this type.

A detailed study of confined diffusion flames includes elements of chemical kinetics, aerodynamics and the transport of mass and heat. To predict the detailed behaviour of such a system it would be necessary to solve the equation of state, the kinetics equations and transport equations of change together with the appropriate boundary conditions. The principal equations of change form a set of nonseparable, nonlinear partial differential equations with boundary conditions which may be very difficult to satisfy. The complexity of this system of equations is horrendous. Even if all these equations were known, which is practically never the case, and we knew a suitable method of solving them on a high speed computing machine, it would be an enormous task. The alternative is, at least from an engineering point of view, to split the problem into parts and to study the influence of particular parameters experimentally. The strict requirements of similarity theory are so numerous that complete modeling of a combustion process is practically impossible and partial modeling is frequently used. Fluid flow is often not greatly influenced by mixing of different species and mixing may be little influenced by chemical reaction. Recognition of such weak influences can be successfully exploited for separate studies of mixing, fluid mechanics and chemical kinetics of combustion processes.

The purpose of this research was to study the applicability of fluid mechanics principles to flame study; namely, to use experimental results on confined incompressible jets and to investigate the influence of the new factors which are introduced to the system when the jet is a diffusion flame. The behaviour of an incompressible, isothermal jet is much better understood than that of jet flames. Recent theoretical and experimental work on such jets, especially that of R. Curtet (7) and its extension, and confirmation by H.A. Becker (3, 4) and J.M. Dealy (8, 9) has led to the establishment of a dimensionless similarity parameter governing certain features of the behaviour of such a jet. This parameter, the Craya-Curtet number, is a function only of the boundary conditions and it has been shown to be the critical factor governing the onset of recirculation, a phenomenon which is of particular interest in flame research. An important question is whether this result can be in some way extended to the case in which the jet is a diffusion flame.

In this thesis an approximate momentum integral analysis is presented to obtain a generalized form of the momentum similarity parameter originally suggested by Curtet, which includes in dimensionless form, the most important new variables introduced to the system by the presence of the flame.

An experimental program was designed in order to obtain more insight into the fluid mechanical behaviour of a confined jet flame, and to test the usefulness of the generalized momentum parameter as a behavioural indicator of such a flame. An effort was made in the design of the furnace to preserve the fluid mechanical boundary conditions of the incompressible flows studied by H.A. Becker and J.M. Dealy. Methane gas was used as the jet fluid because the chemistry of its combustion and its properties are relatively simple and well known. Air was used as the secondary stream. Flow rates of both streams were measured, temperature profiles at different distances above the jet source were recorded, and wall temperatures were measured. In the course of experimental work three different size jets were used with the jet source in turbulent flow and the flame was also always turbulent.

Some typical temperature profiles are presented, and the onset of recirculation as indicated by wall temperatures is discussed.

I

REVIEW OF JET PHENOMENA

Many jet phenomena are qualitatively well understood but are difficult to interpret quantitatively. General discussions and detailed treatments of a number of flows have been collected by Townsend (25), Hinze (13), Schlichting (19), and Abramovich (1). A considerable amount of work done in this field has been devoted to the turbulent jet of incompressible fluid.

Turbulent jets can be classified by their boundary conditions as either free or confined. If a jet is issuing into an infinite medium it is called a free jet, and when the presence of solid boundaries has an influence on the jet flow we refer to it as a confined jet. From a more practical point of view, the ratio of the confinement diameter D_2, to the diameter of the jet source D_1, can be used as a criterion for the type of jet flow to be expected. For free jet flow it is generally necessary that $D_2/D_1 > 100$ and confined jets exist when $4 < D_2/D_1 < 100$. When D_2/D_1 is less than 4, as was shown by Dealy (9), the flow looses its jet characteristics altogether because the jet reaches the wall before it has an opportunity to develop even an approximately self preserving form.

In treating free jets pressure is assumed to be constant throughout the flow field and this results in a basic mechanical difference between free and confined jets.

While in free jets the total integrated axial momentum remains constant from one cross section to another, in confined jets total axial mass flux is preserved and the pressure rises as the jet spreads. Actually, a confined jet is a simple jet pump. The application of confined jet principles to the design of jet pumps stimulated much of the research which has been done on confined jets.

Free turbulent jets are examples of free shear flow and their behaviour is better known than that of confined jets. The presence of a solid boundary complicates the situation somewhat and the flow is no longer free turbulent shear flow. Many experimental data and theoretical results for free jets have, with different degrees of success, been applied to the description of confined jets.

A phenomenon which occurs only in confined jets is recirculation or back flow. In confined jets pressure rises as the jet spreads and if the pressure rises sufficiently before the jet reaches the wall it will reduce the ambient velocity to zero; or in other words, if the pumping effect of the jet exceeds the quantity of fluid available in the secondary flow, recirculation will occur as a stable part of the flow. This confined jet phenomenon is particularly interesting in flame research and furnace design.

Studying confined jet flows, Curtet (7) employed a simple model with the following major assumptions:

flow is nonturbulent outside the jet; wall friction and radial pressure gradient are negligible. In addition, he made use of empirical velocity profile and succeeded in integrating the equations of motion across the mixing tube. The parameters appearing in his final equations were R_2/R_1 and the momentum parameter m. He found experimentally that this momentum parameter is practically a constant of the flow; that is, it does not vary from one cross section to another. The initial value of Curtet's momentum parameter for an axysymmetrical confined jet is:

$$m_o = \frac{R_1^2 \left(U_1^2 - U_2^2\right) + \frac{U_2^2 R_2^2}{2}}{\left(Q_t^2/\pi^2 R_2^2\right)} - \frac{1}{2} \qquad (1)$$

Using his integral analysis, Curtet was also able to compute a critical value of the parameter m_o for the onset of recirculation. Becker studied confined jet type flows extensively using in his experiments a sol-scattered light technique developed by R.E. Rosenweig (3). He made a more general analysis of the flows studied by Curtet and demonstrated the fundamental significance of the Curtet similarity parameter m. Becker suggested a modification of the parameter m_o and called the new parameter Craya-Curtet number giving it the symbol Ct

$$Ct = \frac{1}{\sqrt{m_o}} \qquad (2)$$

He was also able experimentally to determine a critical value of Ct for the onset of recirculation. His experimental value was 0.75.

Dealy (8), in his experiments, used as a jet source fully developed turbulent pipe flow and his data confirmed Curtet's and Becker's results. He has pointed out by means of a simple integral momentum analysis, that Ct is the single parameter governing recirculation in confined jets only if wall friction and radial pressure gradients are negligible, and the confinement is not so severe that the jet can develop its similar form before it reaches the wall. Making use of the Gaussian and cosine distribution,both of which have been found to fit experimental jet velocity profile reasonably well, he was also able to compute the critical value of Ct, and on the basis of the above mentioned assumptions demonstrated why the computed critical values are higher than those observed experimentally.

II

CONFINED-JET DIFFUSION FLAMES

A. General Classification of Flames

Among the wide variety of combustion phenomena, steady flames have received considerable attention. They are important, practically, in a number of applications and significant progress has been made in this field of study since the publication of "Flame and Combustion in Gases" by W.A. Bone and D.T.A. Townend in 1927 (5). An extensive review of combustion bibliography is included in R.M. Fristrom and A.A. Westenberg "Flame Structure" (10). Quickly developing modern experimental technique allows much more insight into the microscopic structure of the flames, and the use of modern computational machines in the theoretical studies offers a better chance of solution of flame equations. However, the complexity of the problem is such that the complete solution has been attempted only for the case of the one-dimensional laminar flame (14).

Flames can be classified with respect to diffusional processes either as premixed flames where fuel and oxidant are premixed before combustion, or diffusion flames where the diffusion of fuel and oxidant and combustion are taking place simultaneously. Most practical flames are diffusion flames mainly because of safety consideration.

By their aerodynamical state, flames can be classified as either laminar or turbulent. It is difficult to define either laminar or turbulent nature of the flame in terms of some critical Reynolds number; whereas, visual differences between laminar and turbulent flame are quite striking. At very low fuel flow rates of, for example, gaseous hydrocarbon, a streamline luminous flame is observed whose length increases proportionally as the fuel flow rate increases. At a certain flow rate, the transition to turbulent flame occurs and the flame shortens while its luminous zone becomes decidedly more diffuse. The addition of turbulence to a flame complicates an already complex situation and despite considerable effort, such flames for the most part have defied quantitative description.

Finally, flames can be classified by their hydrodynamic boundary conditions as free, or confined flames. The present investigation deals with confined turbulent diffusion flames.

Most practical combustion chambers, with the exception of those using a bed of fuel, rely on injection of fuel and/or air through openings which are small in comparison with the dimensions of the apparatus. The resulting confined jet flames have, to greater or lesser extent, the characteristics of confined jets and the flow patterns in a combustion chamber can have an important effect on the efficiency of the furnace.

Recirculation is a characteristic of confined jets which can have an important effect on performance of the furnace and has received considerable attention of flame researchers in last years. Thring and Newby (24) studied enclosed turbulent jet flames using cold models and tried to predict combustion length by means of cold models and a similarity theory. They assumed that confined jets behave in the same manner as free jets before reaching the wall, neglecting buoyancy effects. They developed a similarity parameter governing the behaviour of such cold flames. Later work on cold models (3, 4) revealed that the aforementioned similarity parameter is the proper one only for an ideal or point source jet.

Hottel and Sarofim (15) studied the effect of different flame patterns on the gas temperature field and wall heat flux distribution in a cylindrical furnace for different flow models: plug flow; parabolic velocity profile; ducted-jet flow with different recirculation rates using Craya-Curtet number for cold models as the criterion for recirculation. In all cases the effect of temperature gradients, combustion and energy transfer on the flow patterns was neglected.

Hedley and Jackson (11, 12) have discussed recirculation in combustion chambers for various geometries.

They studied theoretically the influence of different levels of recirculation on chemical reaction time and found a reduction in chemical reaction time for any recirculating system compared to a non-recirculating system. From this finding, it was concluded that an optimum recirculation ratio exists in certain systems. In order to make comparisons easier, they suggested a uniform definition of recirculation ratio as the mass flow of recirculated gases expressed as a percentage of the total mass flow.

B. Momentum Integral Analysis of Confined Jet Flame

The proper use of cold or incompressible flow models can supply some useful information about flame behavior. Recirculation is predicted by cold models and occurs in actual furnaces. The mechanical condition for the occurrence of recirculation in confined jet flames is probably much the same as for cold models; as the jet spreads the pressure rises and if it rises sufficiently to reduce the ambient velocity to zero before the jet reaches the wall, recirculation occurs. If in jet flames some degree of similarity is achieved,there is a possibility of predicting the onset of recirculation from inlet conditions only in a similar way as for the cold models.

A simple integral momentum analysis is presented in this chapter which indicates the most important new variables introduced into the system by the presence of the flame. A number of very rough approximations have been made in order that the prediction of recirculation can be made only from furnace design data.

The control volume used in this analysis is shown in the sketch below. It extends from the jet inlet to the point downstream where the jet reaches the wall.

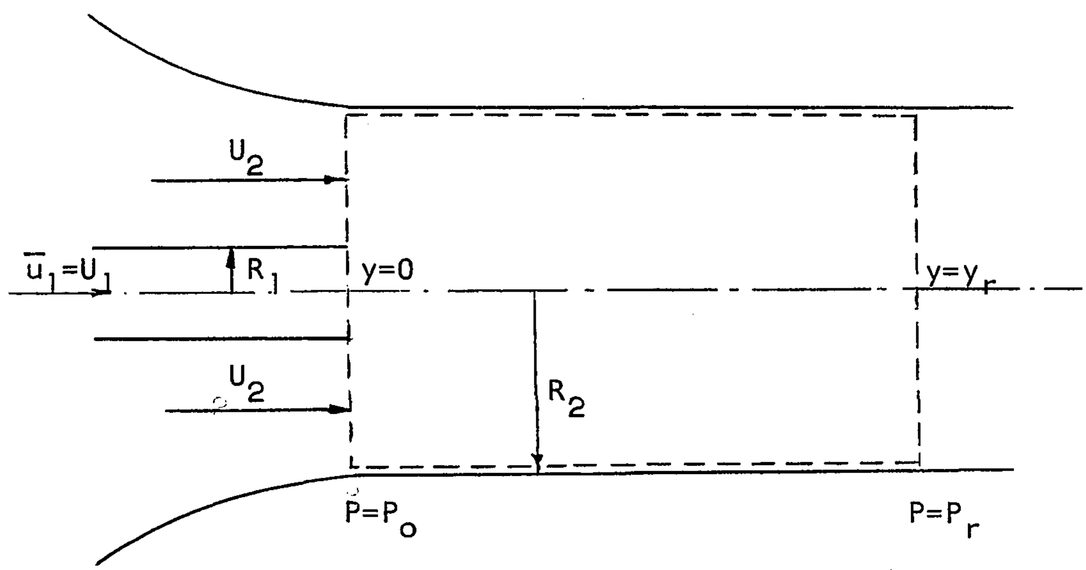

Sketch of Analysis Control Volume

Restrictions on the flow model and some of the pertinent nomenclature are summarized below:

Restrictions: No mole change in reaction, no radial pressure gradient, mixing tube wall insulated. Fuel jet is fully developed turbulent flow. Air flow is non-turbulent and has uniform velocity profile.

Nomenclature:

Fuel denisty	ρ_1
Air density	ρ_2
Adiabatic flame temperature	T_f
Inlet (room) temperature	T_o
Velocity outside the jet	$U(y)$
Axial velocity component	$u(r,y)$
Momentum factor for turbulent pipe flow	β_1

The analysis derived from the equations of continuity and momentum follows:

I Mass Balance:

$$\dot{M} = \rho_1 U_1 R_1^2 \pi + \rho_2 U_2 (R_2^2 - R_1^2)\pi = \int_0^{R_2} 2u\rho\pi r\,dr \Big|_{\text{at any section}} \qquad (1)$$

II Momentum Balance:

momentum flux in is:

$$\rho_1 \beta_1 U_1^2 R_1^2 \pi + \rho_2 U_2^2 (R_2^2 - R_1^2)\pi \qquad (2)$$

II Momentum Balance Cont'd.

momentum flux out is:

$$\int_0^{R_2} \rho u^2 \pi 2 r dr \qquad (3)$$

The pressure force in axial (y) direction is:

$$\pi R_2^2 (P_0 - P) \qquad (4)$$

The overall momentum balance is:

$$2\int_0^{R_2} \rho u^2 \pi r dr - \pi \rho_1 \beta_1 U_1^2 R_1^2 - \rho_2 U_2^2 (R_2^2 - R_1^2)\pi = \pi R_2^2 (P_0 - P) \qquad (5)$$

Bernoulli equation - secondary flow

$$\rho_2 U \frac{dU}{dy} = -\frac{dP}{dy} \qquad (6)$$

Integrating (6) from y = 0 to y = y_r where a virtual recirculation eddy exists (U = 0)

$$\frac{P_r - P_o}{\rho_2} = \frac{1}{2} U^2$$

then applying (5) to the control volume extending from y = 0 to y = y_r and dividing by π

$$2\int_0^{R_2} \rho u^2 r dr - \rho_1 \beta_1 U_1^2 R_1^2 - \rho_2 U_2^2 (R_2^2 - R_1^2) = -\frac{\rho_2 R_2^2 U_2^2}{2}$$

Changing signs, the criterion for the generation of an eddy is that the pressure increase given by (5) be greater than that required to reduce the velocity U to zero

$$\rho_1 \beta_1 U_1^2 R_1^2 + \rho_2 U_2^2 (R_2^2 - R_1^2) - 2\int_0^{R_2} \rho u^2 r dr > \frac{\rho_2 R_2^2 U_2^2}{2} \qquad (7)$$

All the quantities (7) are determined by the boundary conditions except for the third term on the left. Some way must be found to estimate this term from the boundary conditions and the properties of the fluids.

First divide by $\rho_2 U_1{}^2 R_2{}^2$

$$\beta_1\left(\frac{\rho_1}{\rho_2}\right)\left(\frac{R_1}{R_2}\right)^2+\left(\frac{U_2}{U_1}\right)^2\left[1-\left(\frac{R_1}{R_2}\right)^2\right]-\left(\frac{2\int_0^{R_2}\rho u^2 r\,dr}{\rho_2 U_1^2 R_2^2}\right)_r > \frac{1}{2}\left(\frac{U_2}{U_1}\right)^2 \qquad (8)$$

Let

$$\beta_\rho \equiv \frac{2\int_0^{R_2}\rho u^2 \pi r\,dr}{(\dot{M})^2/\rho_2 \pi R_2^2} \qquad (9)$$

β_ρ is a generalized momentum factor for a flow in which ρ as well as u has a transverse gradient. For constant density flow it is obvious that this reduces to the ordinary definition of β, the momentum correction factor.

Then the third term on the left becomes

$$-\frac{(\dot{M})^2\,\beta_r}{\pi^2 U_1^2 \rho_2^2 R_2^4}$$

Inserting this in (8) and rearranging, we have

$$\frac{\beta_1\left(\frac{R_1}{R_2}\right)^2\left(\frac{\rho_1}{\rho_2}\right)+\left(\frac{U_2}{U_1}\right)^2\left[1-\left(\frac{R_1}{R_2}\right)^2\right]-\frac{1}{2}\left(\frac{U_2}{U_1}\right)^2}{(\dot{M})^2/\pi^2\rho_2^2 U_1^2 R_2^4} > \beta_r \qquad (10)$$

Let the left hand side of (10) be represented by Γ. Then, the criterion for the onset of recirculation is that $\Gamma > \beta_r$. For constant density flow $\Gamma = (m_o + 1/2)$ and the criterion for the onset of recirculation reduces to the condition $(m_o + 1/2) > \beta_r$ or

$$C_t < \frac{1}{\sqrt{\beta_r - \frac{1}{2}}}$$

For the incompressible jet, β_r differs from 1.0 due to non-uniformity of the velocity across the tube. In a jet flame, β_r differs from 1.0 due to both the variation of velocity and density. It is now necessary to make some estimate of β_r. Variations in both velocity and density will tend to make β_r greater than 1.0. Thus, it is fairly certain that $\beta_r > 1$. It will not be possible to predict β_r exactly, as similarity in the (ρu^2) profile cannot be guaranteed; however, an order of magnitude figure can be estimated.

From continuity

$$\int_0^{R_2} \rho u r dr = \frac{\bar{\rho}\,\bar{u}\,R_2^2}{2} = \text{constant} = \frac{\dot{M}}{2\pi} \qquad (11)$$

from equation of state

$$\bar{\rho} = \frac{P\bar{\mathcal{M}}}{RT} \qquad \bar{\mathcal{M}} = \text{average molecular weight}$$

For the methane air flame with nitrogen as diluent, considering only reaction $CH_4 + 2O_2 = CO_2 + 2H_2O$ and neglecting changes in density due to pressure variations in y direction, the equation of state can be reduced to:

$$\frac{\bar{\rho}_r}{\bar{\rho}_o} = \frac{T_o}{T_r}$$

or

$$\overline{\rho_r} = \frac{T_o}{T_r}\,\overline{\rho_o}$$

using this in (11) and rearranging

$$\overline{u}_r^{\,2}\,\rho_r = \frac{(\dot{M})^2}{\rho_o\,\pi^2 R_2^4}\cdot\frac{T_r}{T_o} \qquad (12)$$

Then, β_r may be expressed as follows;

$$\beta_r = \left[\frac{2\int_0^{R_2}\rho\,u^2\,\pi\,r\,dr}{(\dot{M})^2/\rho_2\pi R_2^2}\right]_r = \frac{\overline{u}_r^{\,2}\,\overline{\rho}_r\,\pi\,R_2^4\,\rho_2}{(\dot{M})^2}$$

Using (12), a simpler expression for β_r can be obtained:

$$\beta_r = \frac{T_r}{T_o}\cdot\frac{\rho_2}{\overline{\rho}_o}$$

Let

$$T_r\,\frac{\rho_2}{\overline{\rho}_o} = T_f\cdot K \qquad (13)$$

then

$$\beta_r \approx K\,\frac{T_f}{T_o} \qquad (14)$$

Constant K must be determined experimentally.

This result plus equation (10) gives an approximate criterion for the onset of recirculation based solely on the inlet conditions of the flow and some simple properties of the fluids involved. This criterion is

$$\Gamma > K \frac{T_f}{T_o}$$

or $$\left[\frac{\Gamma T_o}{T_f}\right] > K$$

III

EXPERIMENTAL EQUIPMENT

A. Description of Equipment:

There were two basic requirements for the experimental design; the experimental system had to be consistent with the model employed and it had to produce a stable turbulent flame.

Figure (1) is a schematic diagram of the equipment and figure (2) shows an overall view of apparatus. Air was blown by a variable speed blower through a metering orifice and a gate valve through the double inlet into the flow conditioning section. In the course of the experiments three different orifices were used, giving 7" water differential pressure for flow rates 50, 15 and 7.5 SCFT/min. The air flow was regulated by a gate valve mounted in the 2" pipe 18" downstream from the metering orifice. Methane gas (Matheson, Technical grade min. 97% purity) from cylinders was used as the jet fuel. Two calibrated rotameters were used to cover the measured range of the fuel flow. As the jet sources, three thin-wall stainless steel tubes were used with I.D. of 0.100", 0.145" and 0.179". All the tubes were sufficiently long that a fully developed turbulent velocity profile was assured at the jet source. Because of the small diameter of the jet tubes and experimental difficulties with flame stabilization at very high fuel velocities, only relatively low

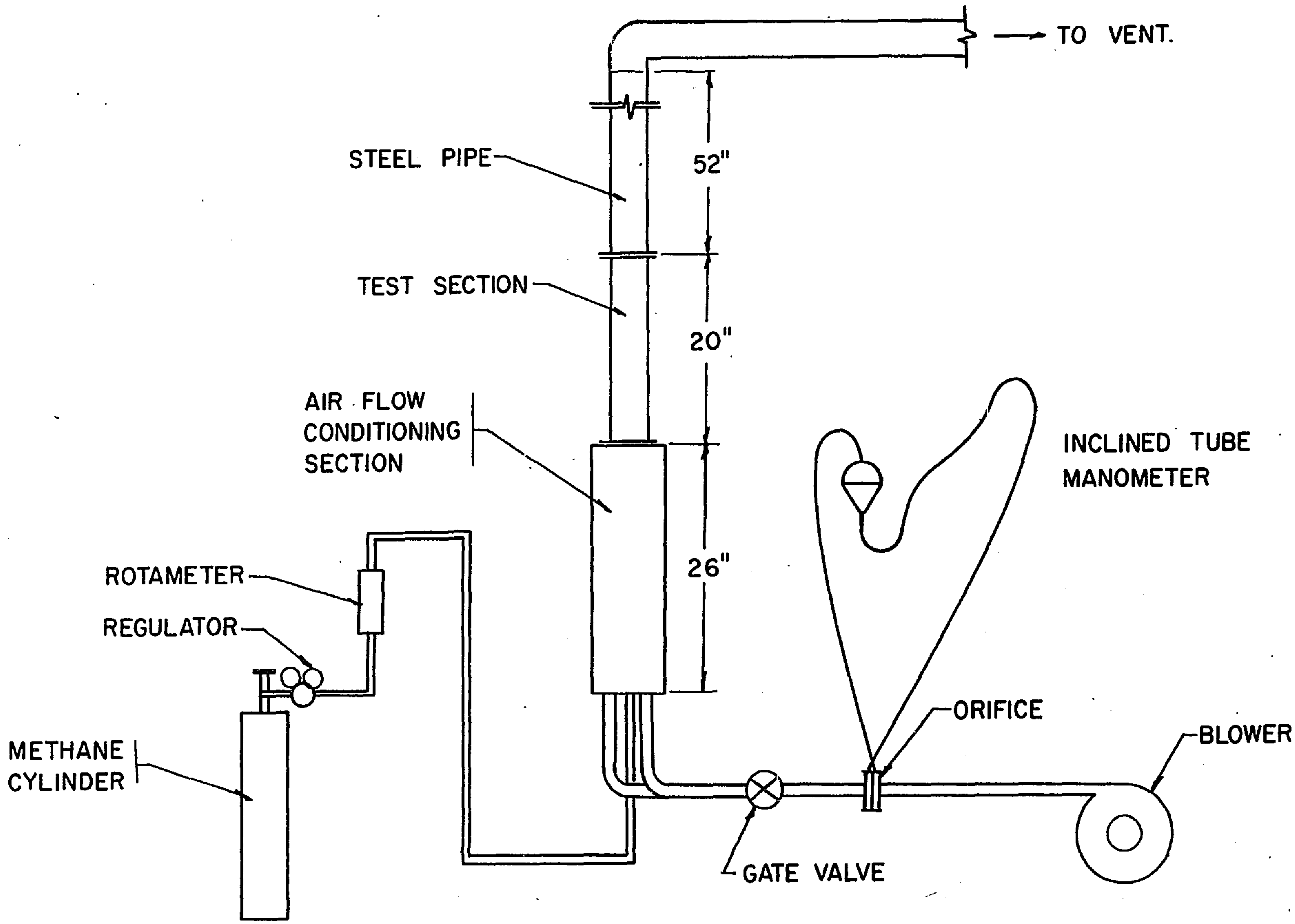

FIGURE I. SCHEMATIC DIAGRAM OF THE EQUIPMENT

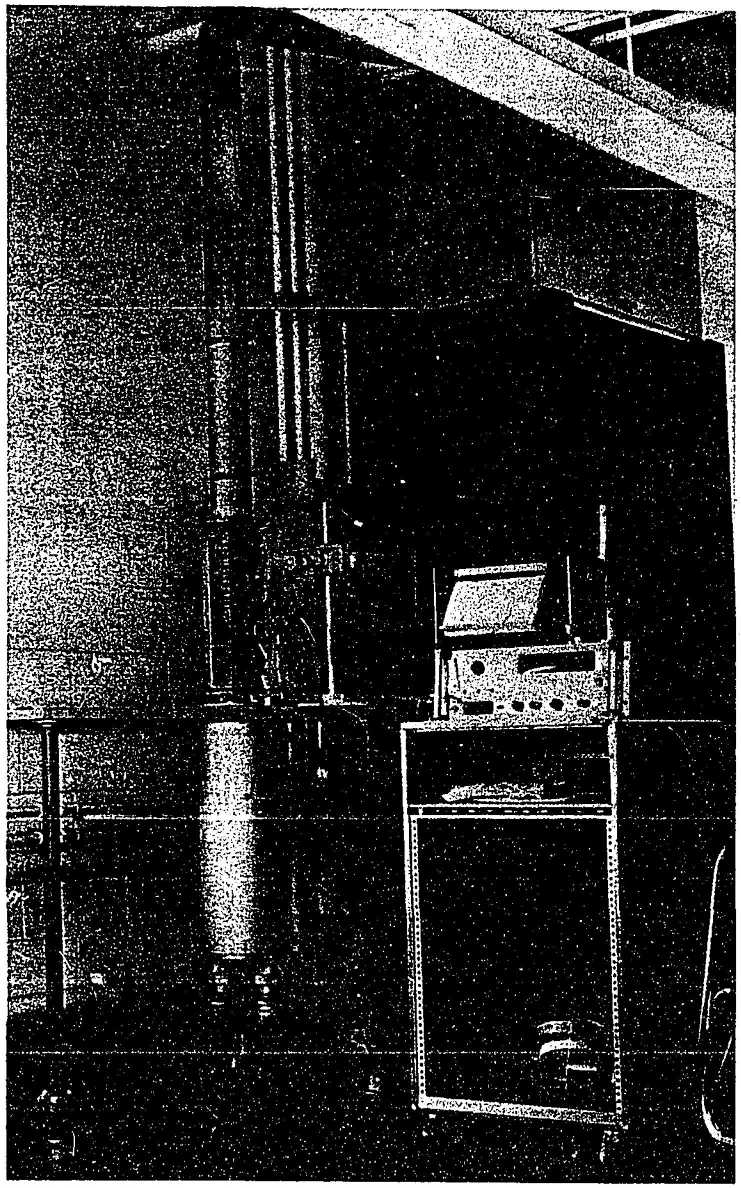

Figure 2: Overall View of Apparatus

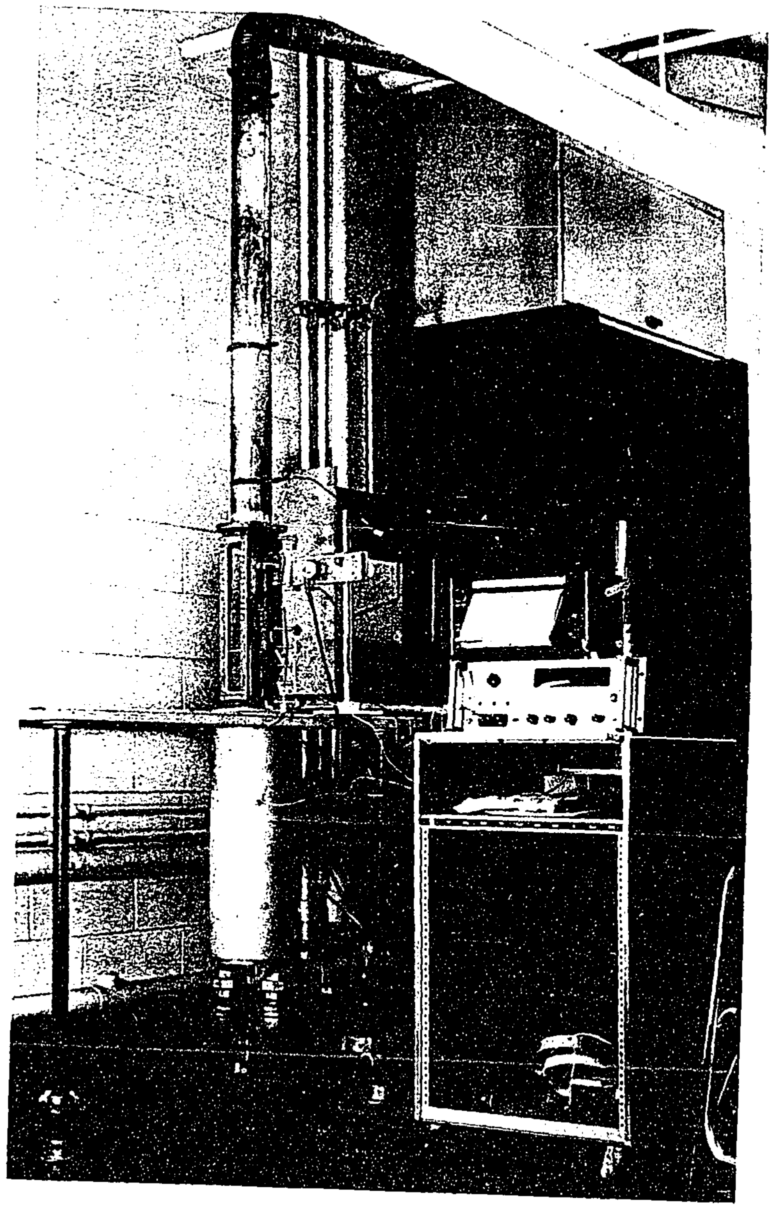

Figure 2: Overall View of Apparatus

jet tube Reynolds numbers were studied (3000 - 5000). However, the resulting flames were in all cases clearly turbulent. As the fuel flow rate was raised to the operating rate, laminar flames were observed, but they always became turbulent at the operating conditions. The fuel flow discharged into a secondary air stream in cocurrent flow at the bottom of 20" long 4" I.D. test section made from stainless steel. Three 2" wide and 16" high windows of Vycor glass were built in at the three sides of the section. The test section was followed by a 25" long mild steel pipe of the same I.D. as the test section. Above this, stove piping was attached leading into the exhaust duct of a fume hood.

B. Air Flow and Hot Wire Measurements:

The boundary conditions in the hydrodynamic model employed were that the air flow was nonturbulent and its velocity profile was uniform. To get experimental flow conditions as close as possible to these requirements, a flow conditioning section was designed. Figure (3) shows this section.

Air entered the section at the bottom, went through four perforated plastic plates, through a honeycomb and through a converging section 8" long having a diameter decreasing from 8" to 4". The conditioning section was made of aluminum and the converging section was machined

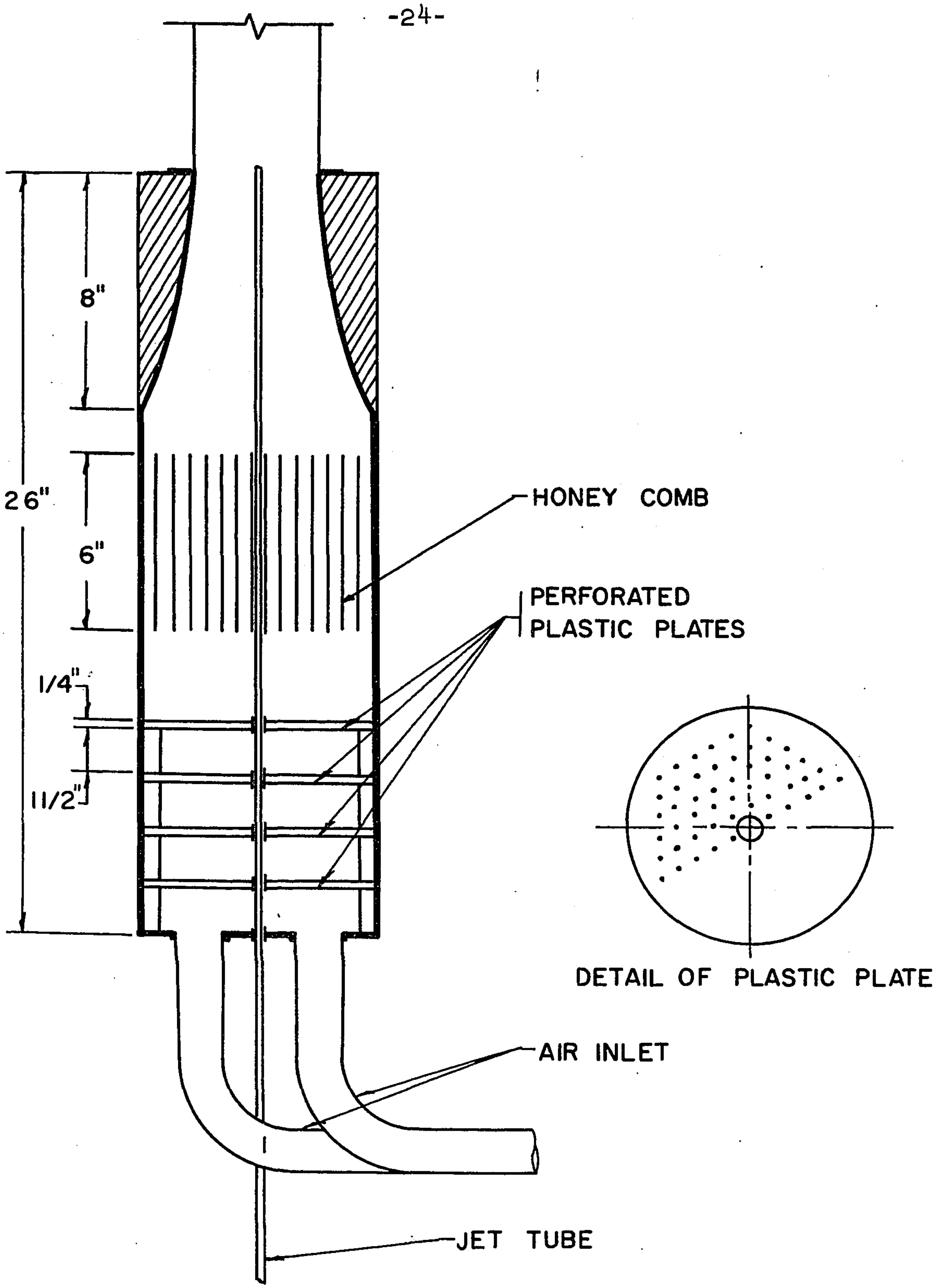

FIGURE 3. AIR FLOW CONDITIONING CHAMBER

from aluminum stock. Four perforated plastic plates at the bottom of the section 1.5" apart served as air flow distributors. There were 90 holes drilled in each plate. The holes were symmetrically spaced but the diameter of the holes varied from 1/8" to 1/2". The effects of different hole sizes and distributions were tested at the entrance to the test section by measuring the velocity profiles with a total head tube mounted on a traversing mechanism. This procedure was repeated several times until a satisfactory velocity profile was obtained. These tests were carried out at higher velocities than those employed in the actual experiments. To check the velocity profiles under operating air flow velocities, a constant temperature hot wire anemometer was used.

Figure (4) is a photograph of the instruments used to determine the air inlet velocity profile. The constant temperature anemometer used was a DISA model 55A01, which gives voltage outputs proportional to the time-averaged velocities. The output of this instrument was measured by a digital voltmeter. The probes used were type 55 A 22 gemeral purpose DISA hot wire platinum plated tungsten probes (D wire 0.005 mm, operating length $\approx$ 1 mm). The hot wire probes were calibrated in a round-edge orifice-type calibration unit. A detailed description of the calibration unit used is given elsewhere (6). Figure (6) shows velocity profiles at the air flow rates 5, 10 and

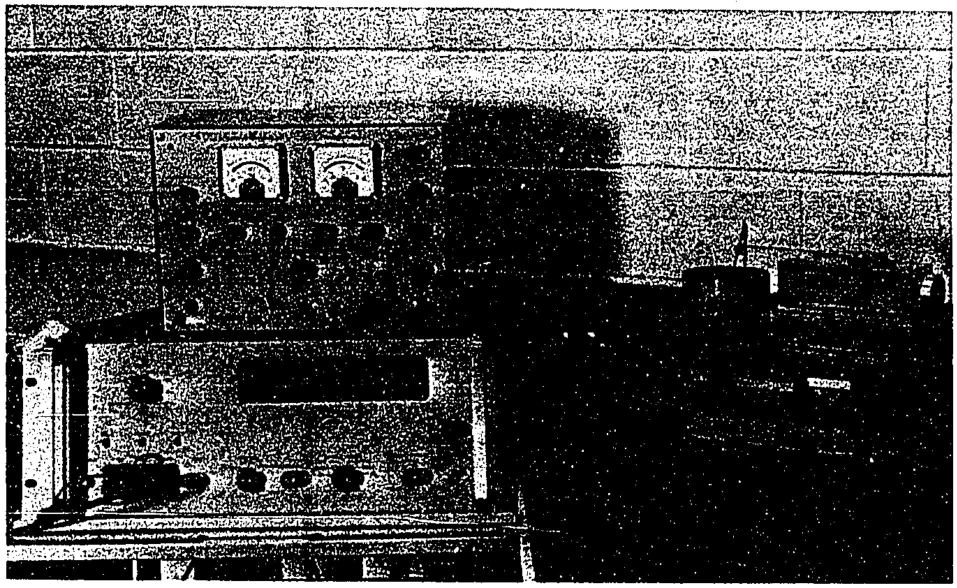

Figure 4: Equipment for Air Inlet Velocity Profile Measurement

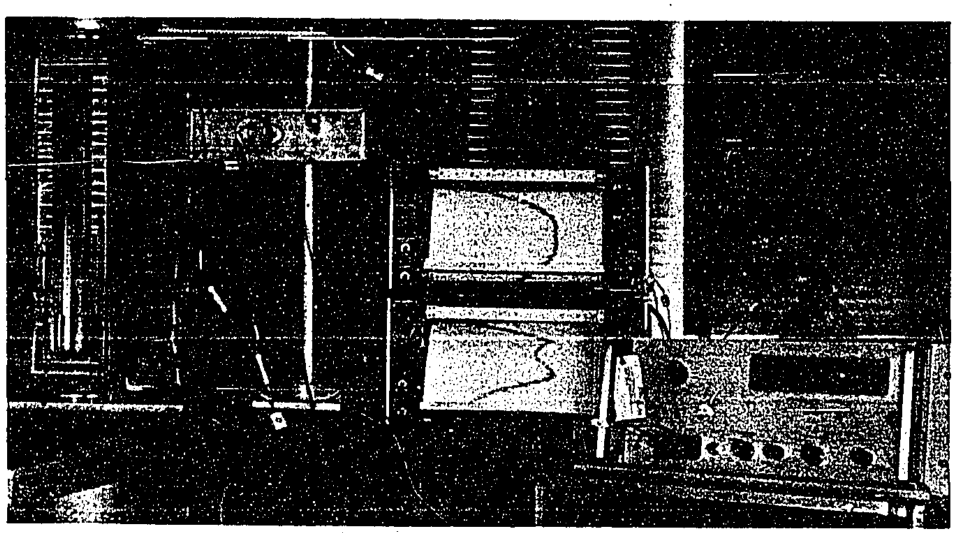

Figure 5: Test Section and Instrumentation for Temperature Measurements

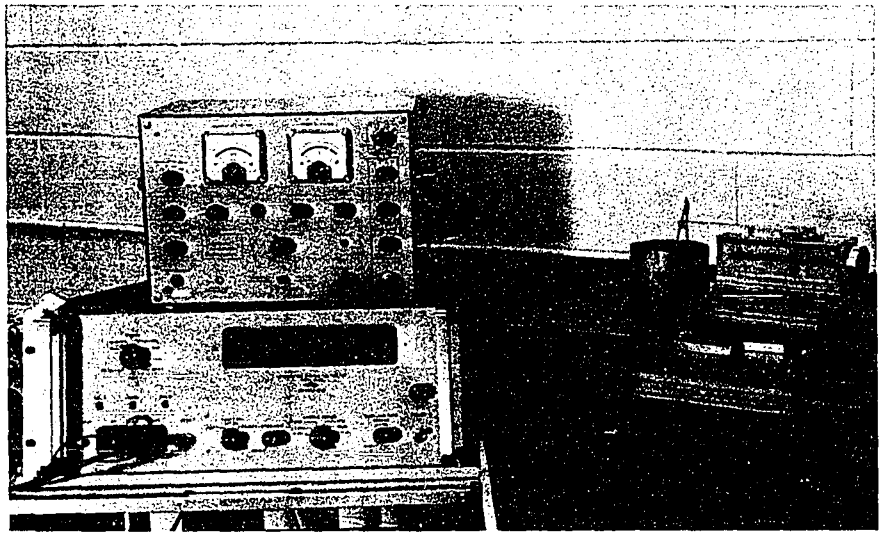

Figure 4: Equipment for Air Inlet Velocity Profile Measurement

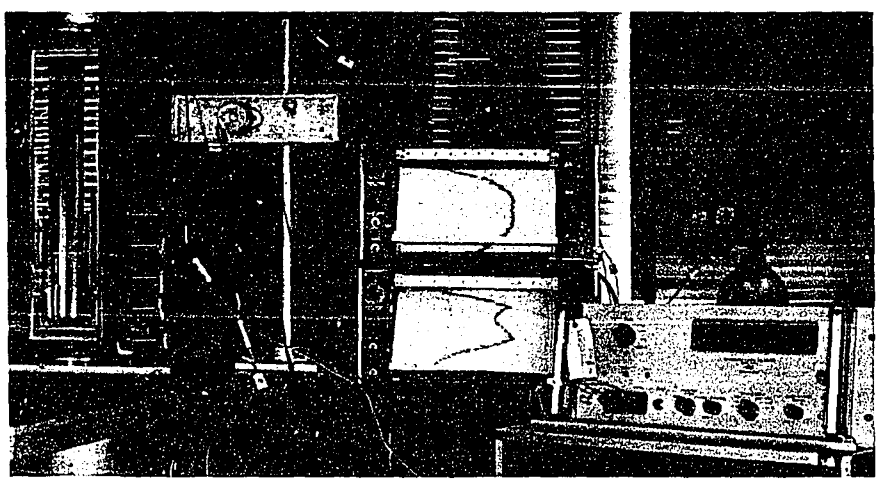

Figure 5: Test Section and Instrumentation for Temperature Measurements

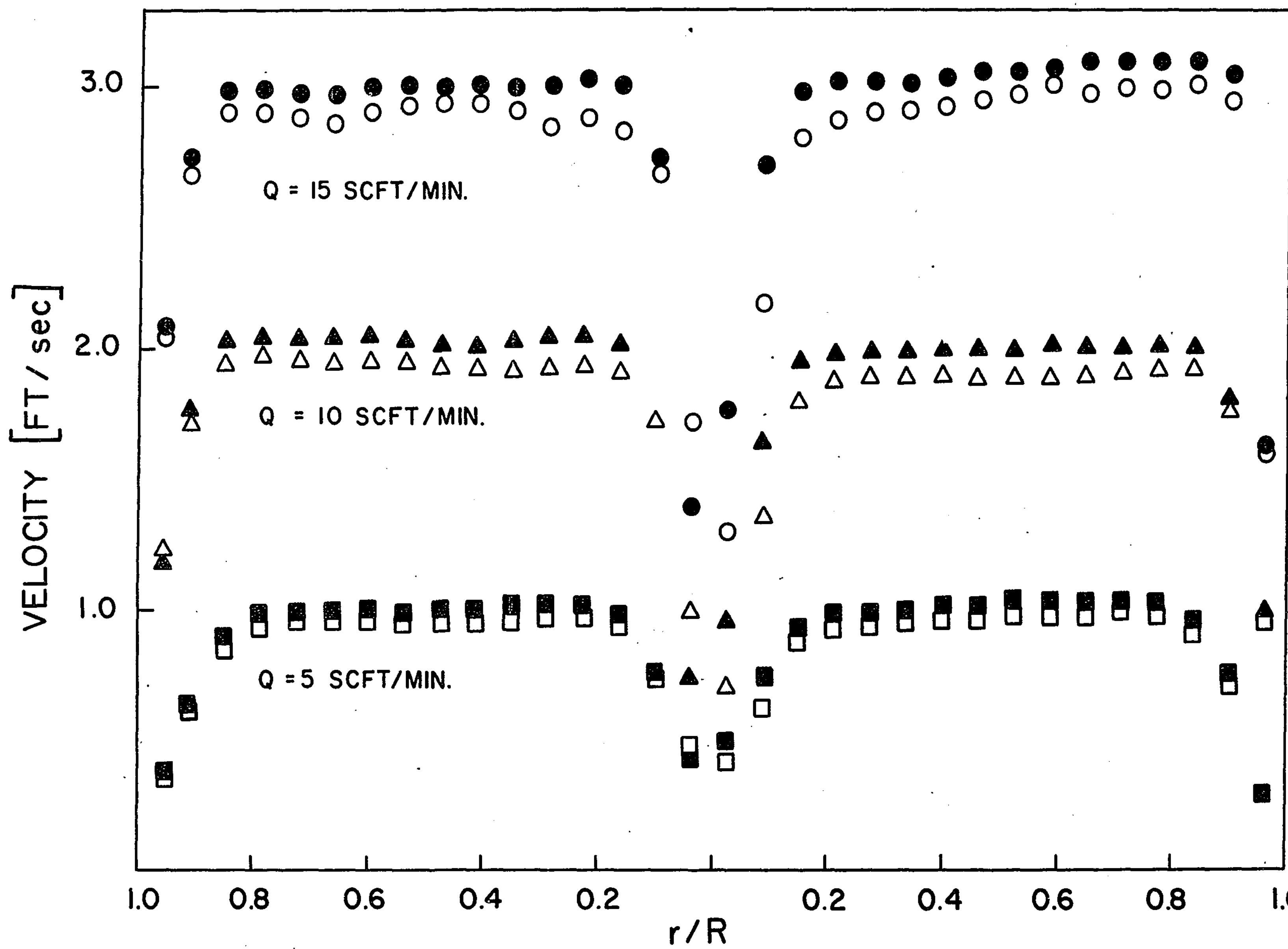

FIGURE 6. AIR VELOCITY PROFILE AT FURNACE INLET – NO FUEL FLOW

15 SCFT/min. Each profile traverse was taken across two mutually perpendicular diameters of the cross section.

C. Flame Stabilization:

Flame stabilization is of vital importance in most applications of flame technology. A significant part of the combustion literature is devoted to this problem. A general treatment and many practical guides are given by Lewis and von Elbe (17).

However, it proved to be difficult in these experiments to stabilize the high velocity turbulent diffusion flame with air supplied by blower in such a way as to avoid flow disturbances. A loop of electrically heated platinum wire was used as shown in figure (7). The heated loop also served as an ignition device. Wires were often burnt and had to be replaced, but no differences were observed in the appearance of the flame when the wire diameter or loop shape were changed. Wire diameters were 0.007" and 0.010" and they were made of platinum or platinum with 10% iridium.

D. Temperature Measurements:

In order to obtain more information about the flow regime in the furnace, temperature profiles and wall temperatures were measured at different distances in the test section above the jet source. A schematic diagram

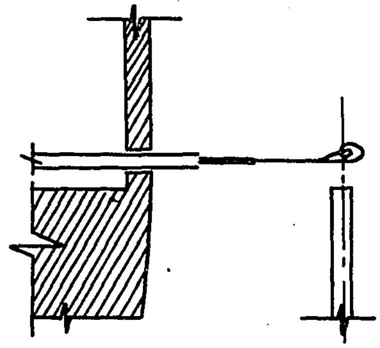

DETAIL "A" SECTION

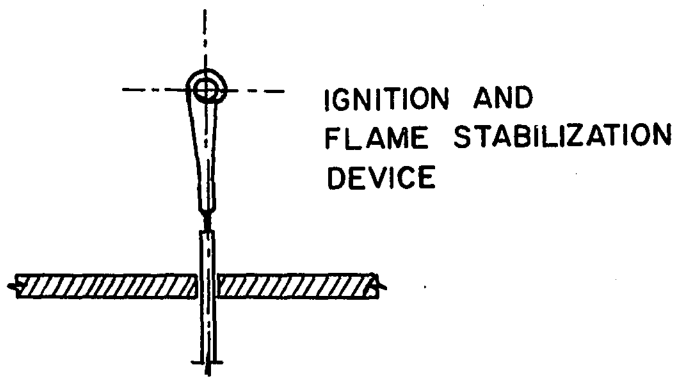

DETAIL "A" PLAN

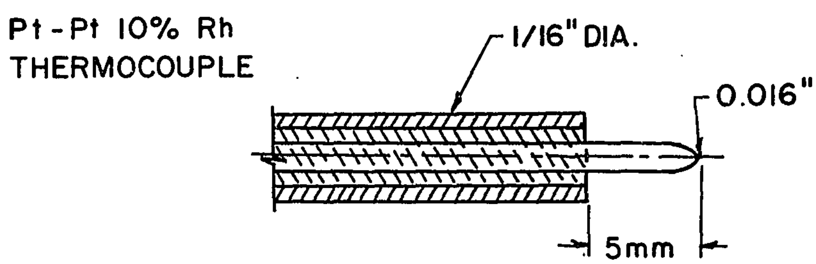

FIGURE 7. DETAILS OF APPARATUS

of test section is shown in figure (8).

To measure wall temperatures four Chromel-Alumel thermocouples were built into the wall of the furnace at heights above the jet inlet of 6", 11", 17" and 25". Milivolt outputs were recorded on a Moseley strip chart recorder model 7100B. Temperature profiles were also measured at four different locations in the test section; 4", 8", 13" and 18" above the jet inlet. For this purpose a Pt-Pt 10% Rh thermocouple probe was mounted on the constant speed traversing unit shown in figure (5). The traversing unit consisted of a small synchronous 1. RPM motor with appropriate gears. This device provided a traversing speed of 1"/min. The thermocouple probe 8" long and 1/16" in diameter, consisted of thermocouple wires, Al_2O_3 packing surrounded by a platinum shield. The last 5 mm of the thermocouple wires together with the junction were exposed as shown in figure (7). The size of the junction was 0.016". The thermocouple extension wires were connected to the same type of recorder used for wall temperature measurements. Continuous curves were obtained in this manner. The milivolt records thus obtained had to be converted to temperature and corrected for the radiation error. Knowing the speed of the probe movement and that of the recorder chart paper, radial distances corresponding to any point on the curve could easily be found.

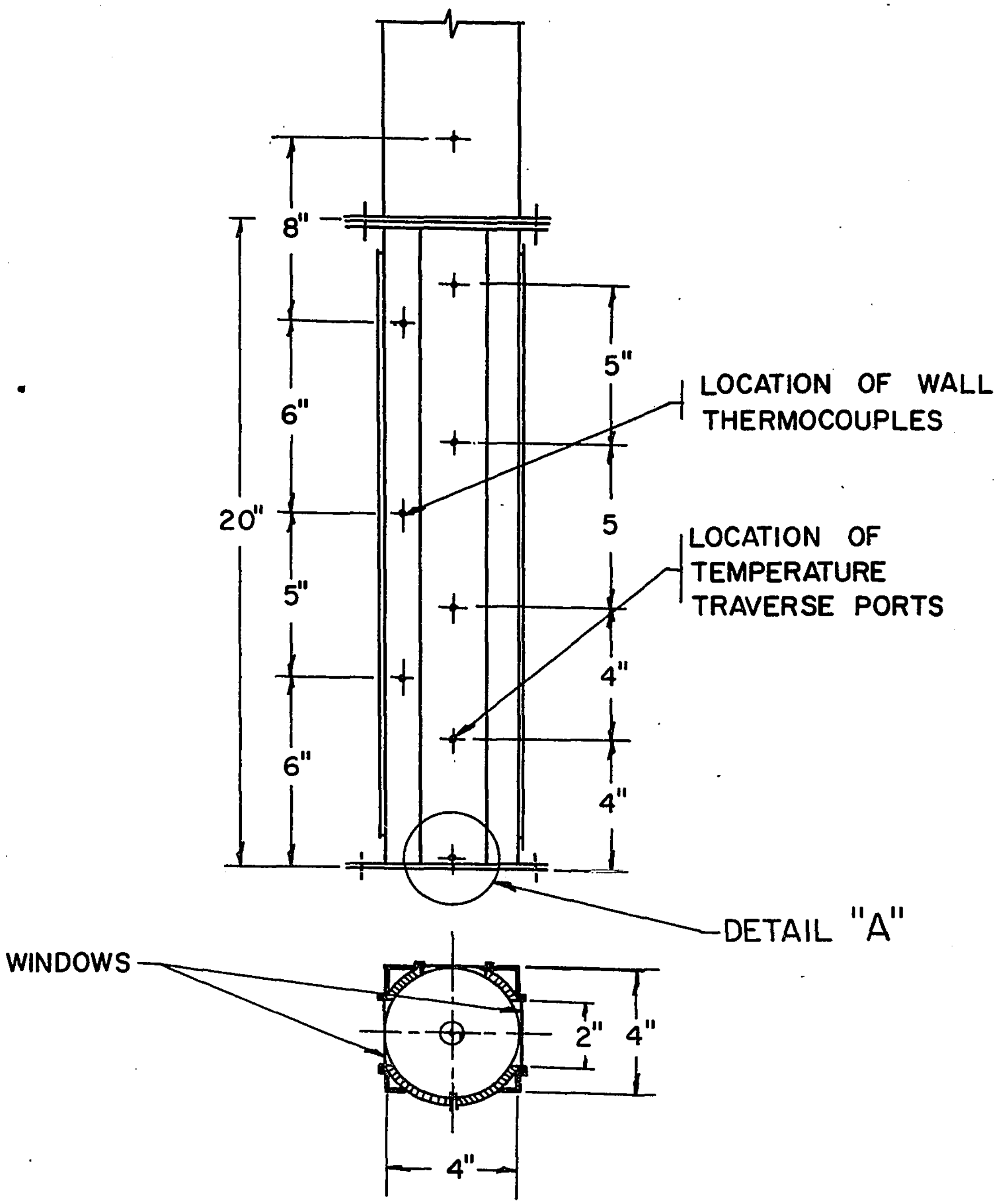

FIGURE 8. TEST SECTION

E. Temperature Corrections:

For point temperature measurements inside the flame, small size precious metal thermocouples are widely used. The main disadvantages in the use of this type of measurement are errors due to the catalytic effects of the thermocouple itself, radiation and heat conduction errors, and the errors due to the difference between the static and the total temperature of the hot gases.

At moderate velocities ($M<0.1$) the last effect mentioned can be neglected (2). With the proper design of the probe, radiation errors far exceed the errors due to the heat conduction through the thermocouple, and the catalytic effects were minimized by coating the thermocouple with a thin homogeneous layer of silica. The coating technique was in principle the same used by previous workers and is described in more detail elsewhere (10). For this "flame plating" a blast burner supplied with natural gas and compressed air was used. The silicone compound used was Union Carbide L-45 silicone oil. To obtain uniform coating, the thermocouple was moved through the flame by the same constant speed driving unit used for temperature profile measurements. The temperature of the coating was measured by the thermocouple being coated. The quality and the thickness of silica layer were examined with a microscope. Finally temperatures in the methane flame as indicated by the coated Pt-Pt 10% Rh thermocouple were compared to those indicated by a Chromel-Alumel thermocouple of the same size, for which no catalytic effects have been reported (22).

Measured temperature profiles were corrected for radiation error. Radiation error can be estimated by equating heat transferred to the probe from the gas to that part by radiation (16). Neglecting radiation from surrounding walls and from hot gases to the thermocouple, a relation of the following form was obtained;

$$\Delta T_{rad} = \frac{\epsilon\sigma}{\alpha} T_w \qquad (1)$$

where ϵ is emissivity of the thermocouple's surface, σ is Stephan-Boltzmann constant, α a heat transfer coefficient and T_w the measured temperature as indicated by the thermocouple. The value 0.22 for ϵ was obtained from the literature (16), and the value of α was estimated on the basis of the heat transfer correlations for cylinders. The Reynolds numbers based on the diameter of the thermocouple junction were between 3 and 9.

Correlations available from literature (18) were valid for Re numbers 1 - 4 and 4 - 40. Those were plotted and a new straight line was drawn in between to obtain coefficients which were used for the operating range. The correlation thus obtained was

$$Nu = 0.85 \, Re^{0.36} \qquad (2)$$

where Nu is the Nusselt number

combining (1) and (2)

$$\Delta T_{rad} = \frac{1.18 \times \epsilon \times \sigma \times D^{0.64}}{\lambda} \left(\frac{\mu}{\rho u} \right)^{0.36} T_w^{\,4} \qquad (3)$$

Where D is a diameter of the thermocouple junction, μ is viscosity, ρ density, u velocity and λ heat conductivity, all at the flame temperature. The thermal conductivity of air was obtained by extrapolating the data available from the literature (23).

For density and viscosity also, values for air were used. Lacking the data for (ρu) profiles it was decided to use the air velocity in uniform profile for the calculation of temperature corrections. This approximation obviously gives values of ΔT_{rad} which are too high, primarily because the highest temperature region was the jet region, where actual velocities were higher. This effect was enhanced with the decreasing size of the jet. To simplify calculations and partially to compensate for this effect, it was decided to use the air flow velocities for the largest jet (0.179 I.D. and air equivalent ratio 1.5) for all jets. Values of ΔT_{rad} were computed for different jet tube Reynolds numbers, and plotted versus measured temperature. Flame temperatures were then obtained by adding ΔT_{rad} to the measured temperature.

IV

EXPERIMENTAL RESULTS

Three different jet velocities were studied in the case of the 0.145" and 0.179" diameter jets and two for the 0.100" diameter jet. The air equivalent ratio varied from 1 to 2 in all cases. In each of the 55 experiments temperature profiles and wall temperatures were measured at all measuring points in the following way. At first only air was blown through the furnace to obtain a stable reading on the inclined manometer connected to the pressure taps of the metering orifice. The methane cylinder valve was opened and the methane gas was ignited by the electrically heated platinum wire. When the wall temperature indicated by the thermocouple 25" above the jet inlet was just above 100°C, the methane gas valve was closed and the furnace was allowed to cool down slowly to a temperature just below 100°C at the same measuring point. Then the methane gas was ignited again and adjusted to the operating flow rate. When the wall temperature reached exactly 100°C the traversing mechanism for the thermocouple probe and both recorders were switched on at the same time. For each of the 55 experiments the procedure was repeated four times to obtain four temperature profiles and four wall heating rates.

Temperature profiles are presented in figures 9 - 22. Typical sets of data were chosen to cover the range of variations of jet tube diameter, jet tube Reynolds number and air equivalent ratios being studied.

Wall heating rates as indicated by wall temperature measurements are presented in figures 23 and 24. In figure 23 the ordinate is the dimensionless heating rate $\left(\frac{\Delta T}{\Delta t}\right)\left(\frac{D_m}{U_2 T_f}\right)$ where D_m is the diameter of the mixing tube, U_2 the air inlet velocity, T_f the adiabatic temperature of the flame, ΔT the temperature difference between initial and final temperature measured in the time interval Δt. The abscisa is Γ defined in chapter II multiplied by the ratio of room and adiabatic temperature of the methane flame for the given value of air stoichometric ratio. In figure 24 the heating rate $\frac{\Delta T}{\Delta t}$ is plotted versus dimensionless distance above the jet inlet $\frac{y}{D_j}$ (D_j is the diameter of the jet tube and y the distance above jet inlet) for different values of Γ and constant jet tube Reynolds number.

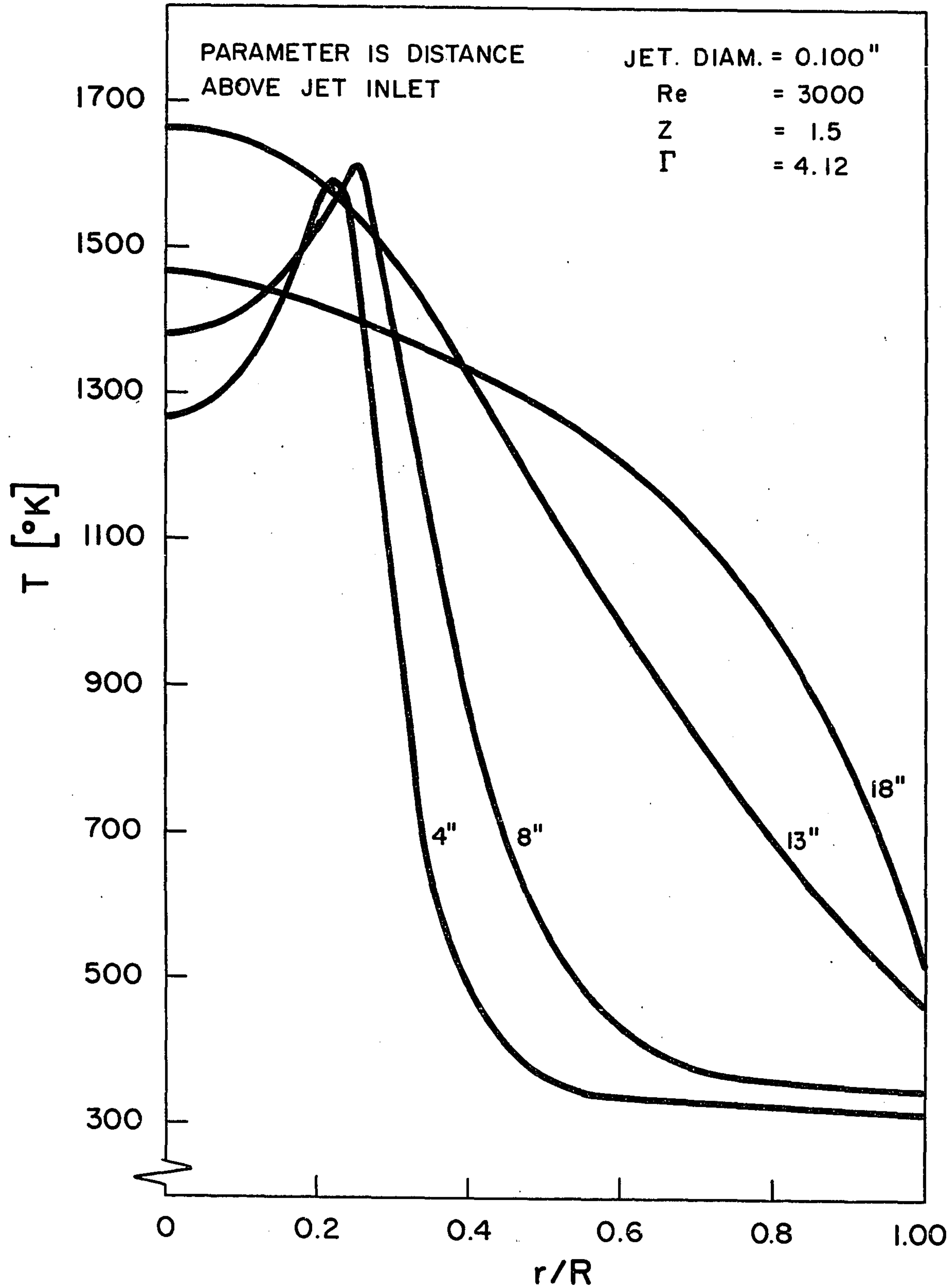

FIGURE 9. TEMPERATURE PROFILES

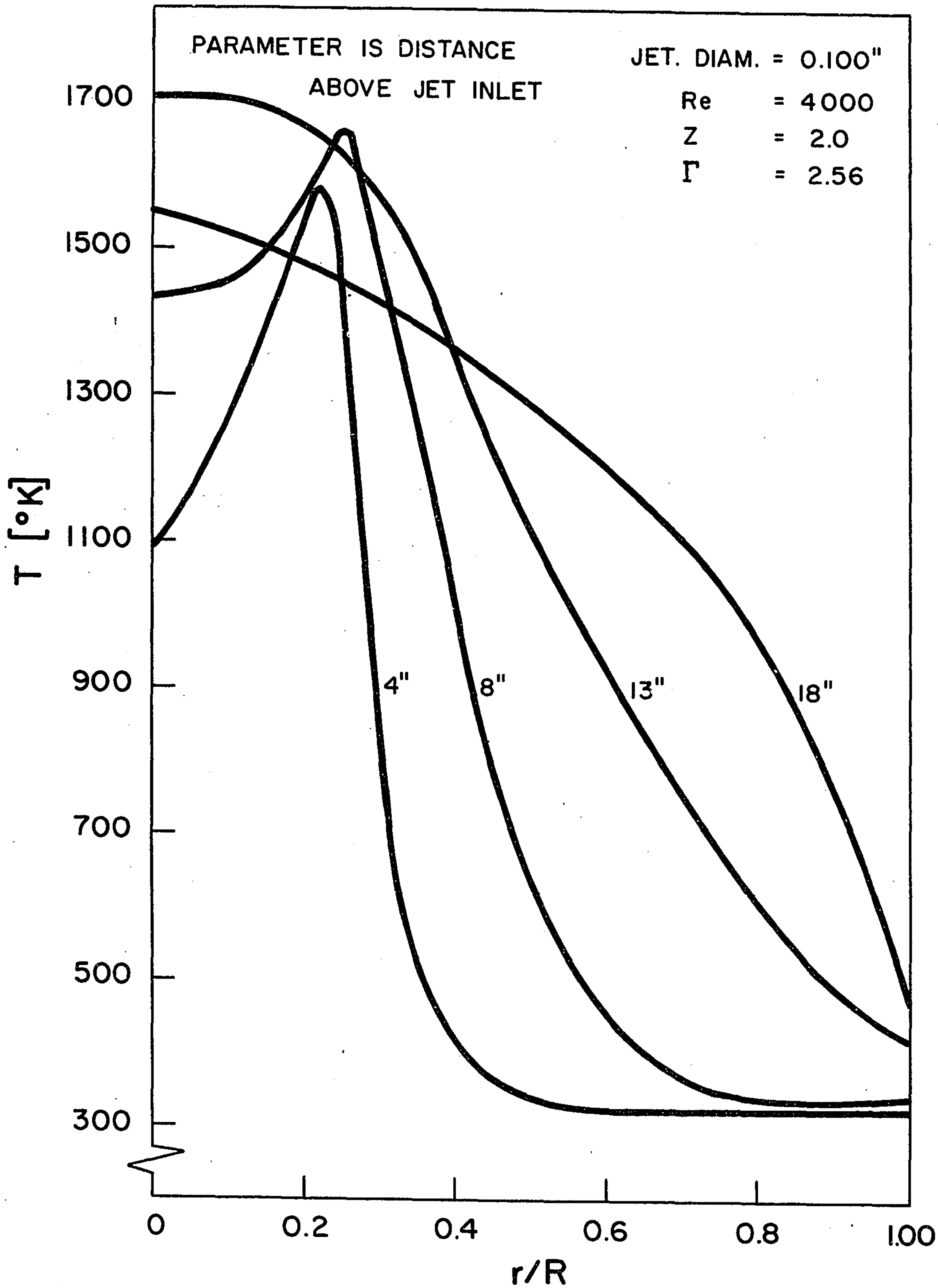

FIGURE 10. TEMPERATURE PROFILES

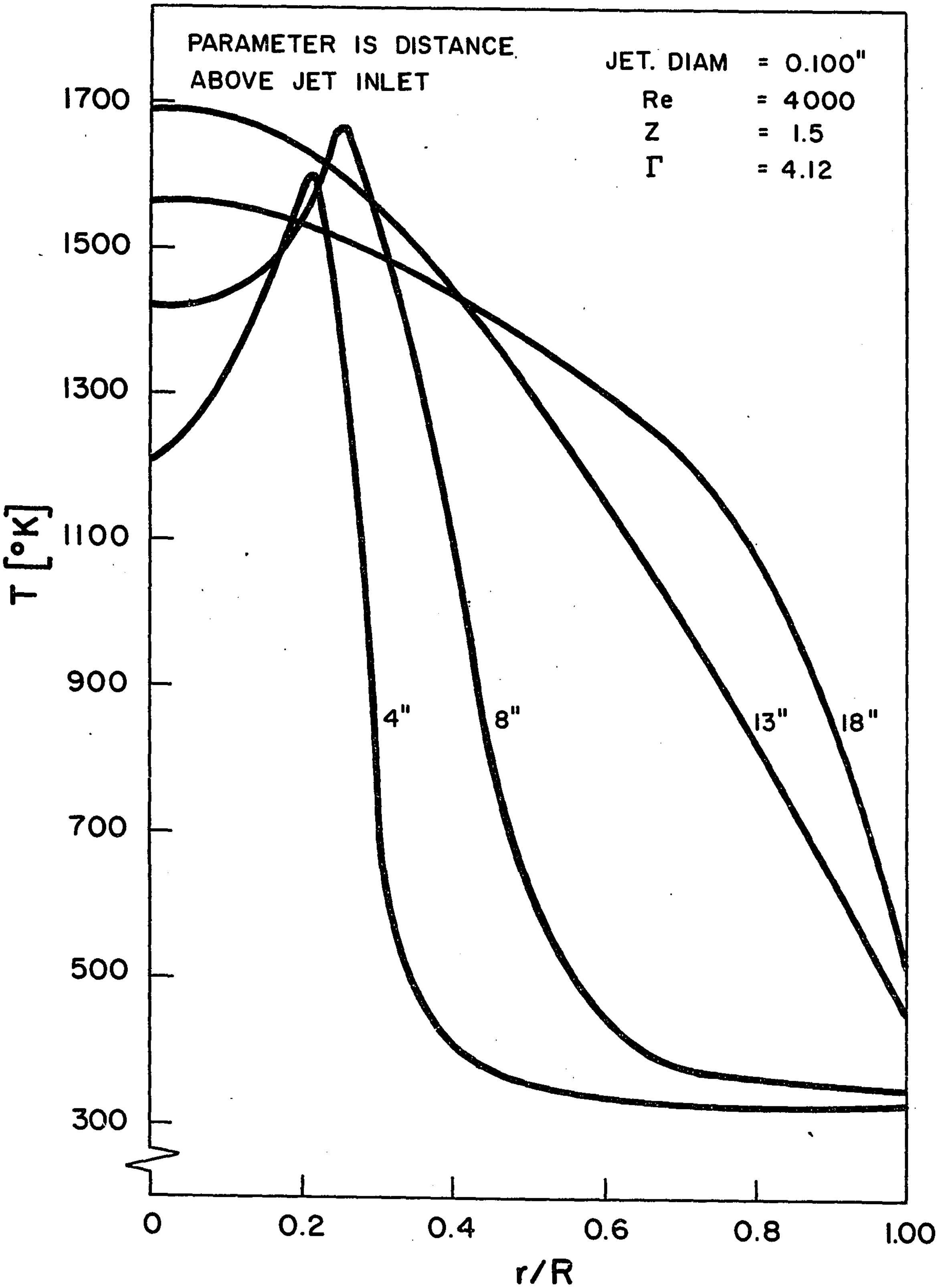

FIGURE 11. TEMPERATURE PROFILES

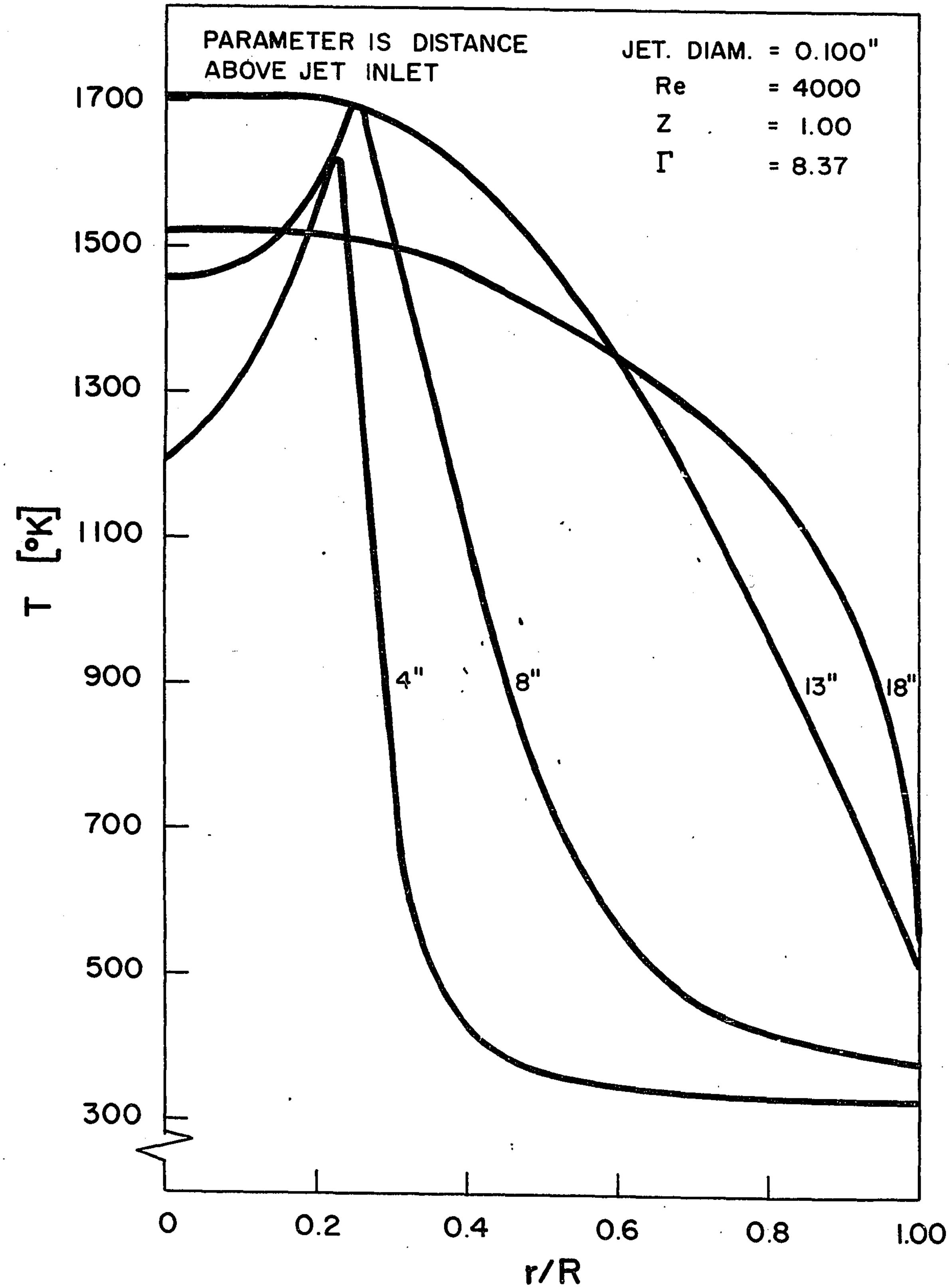

FIGURE 12. TEMPERATURE PROFILES

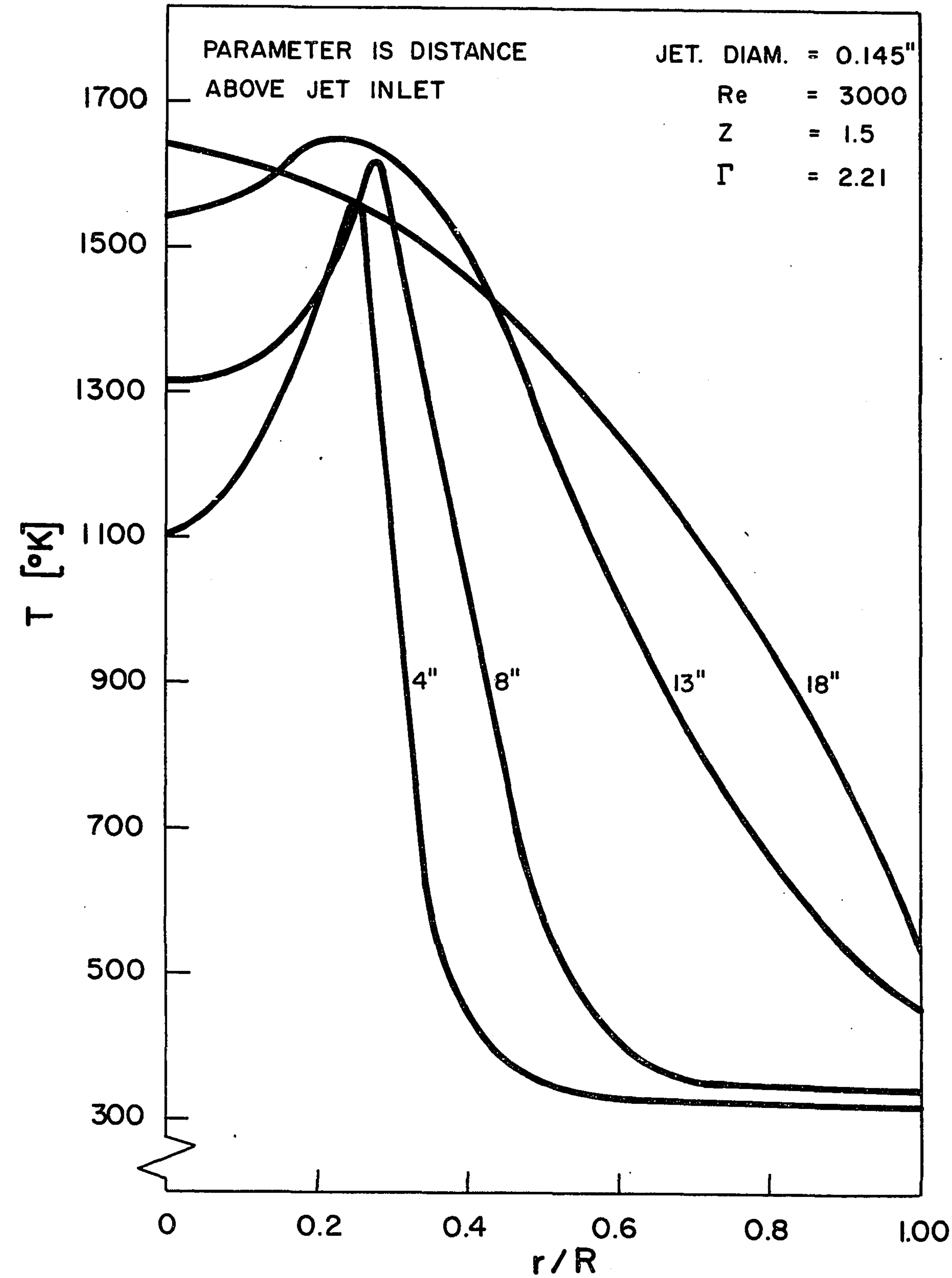

FIGURE 13. TEMPERATURE PROFILES

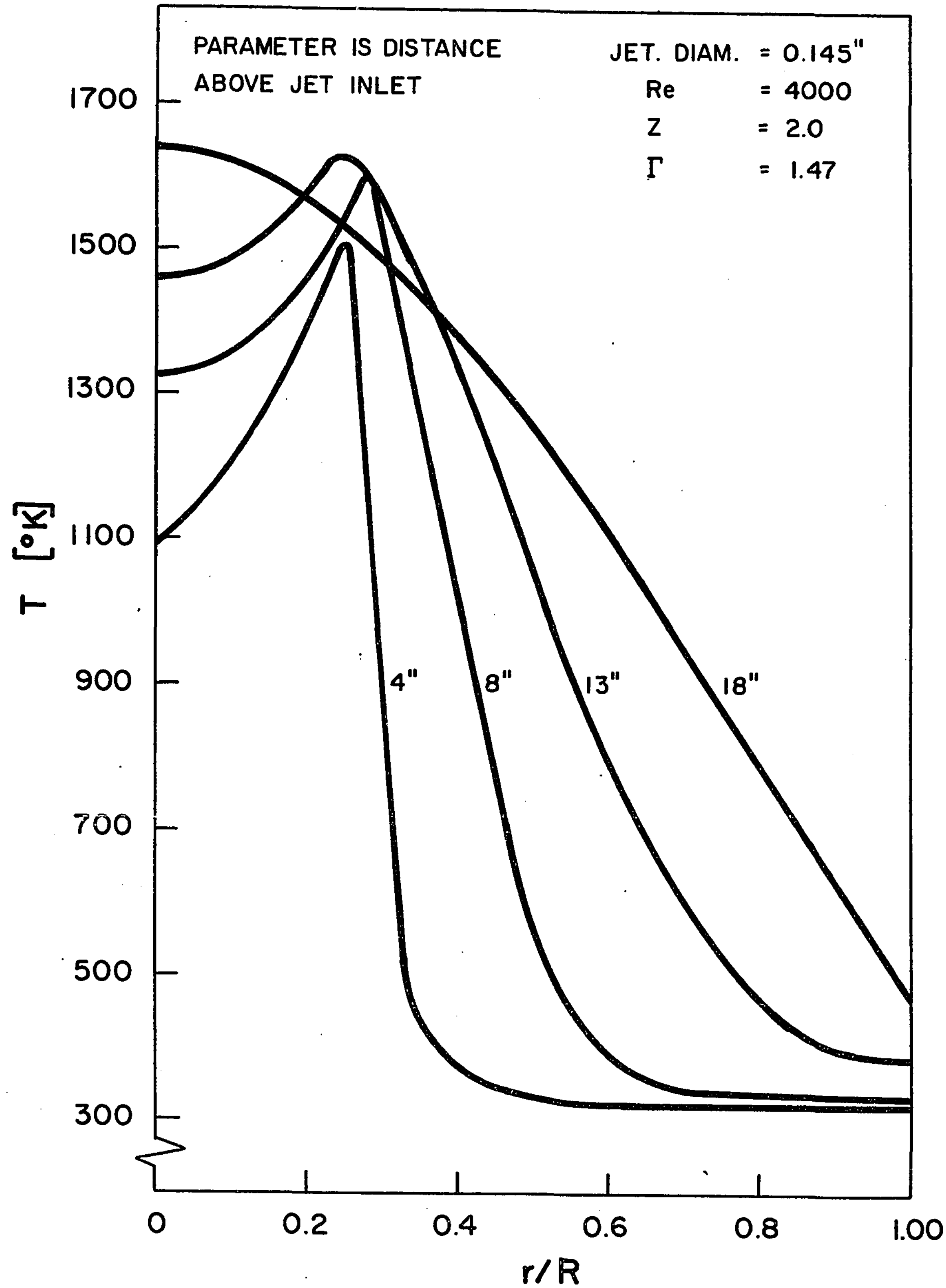

FIGURE 14. TEMPERATURE PROFILES

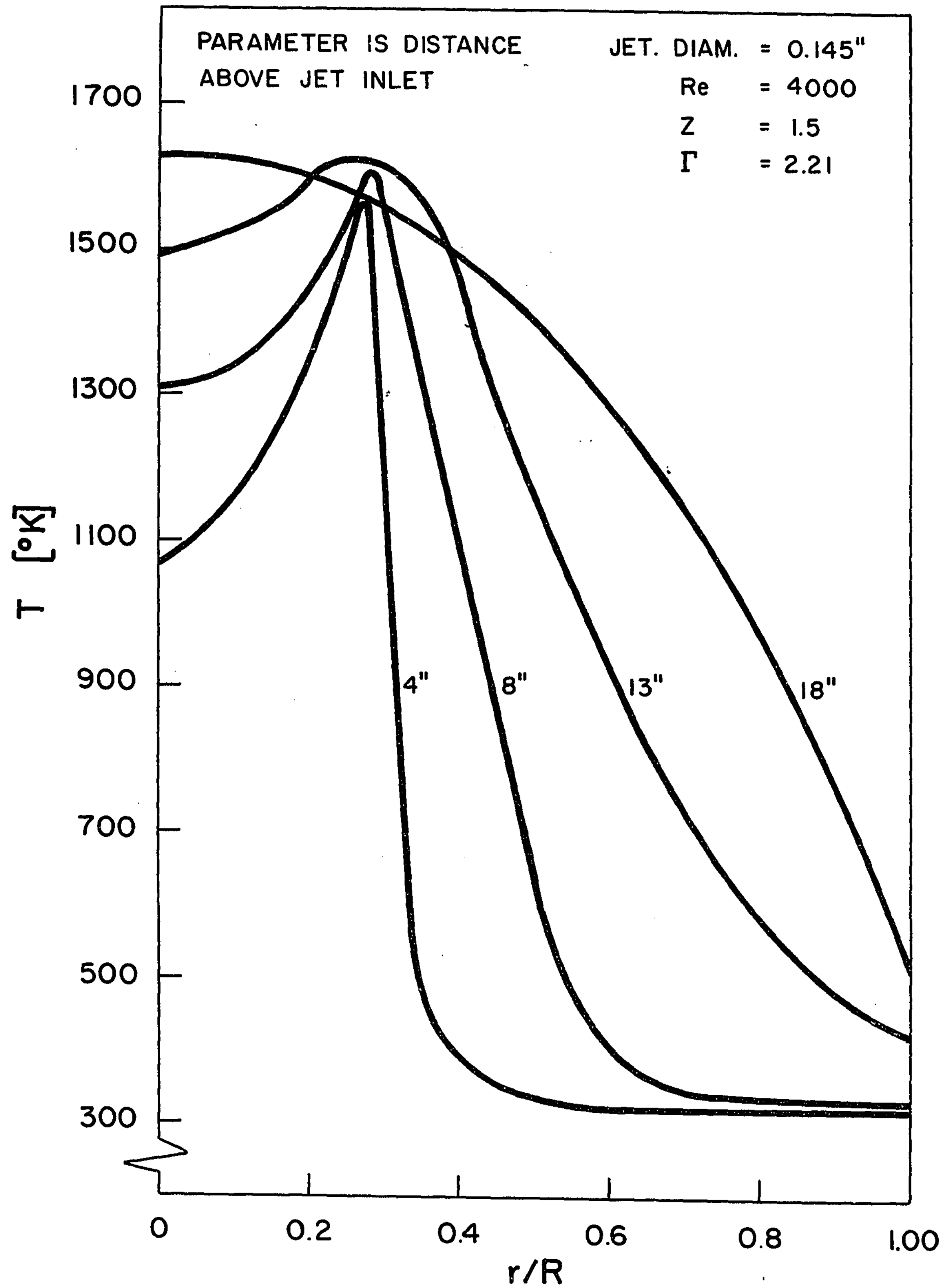

FIGURE 15. TEMPERATURE PROFILES

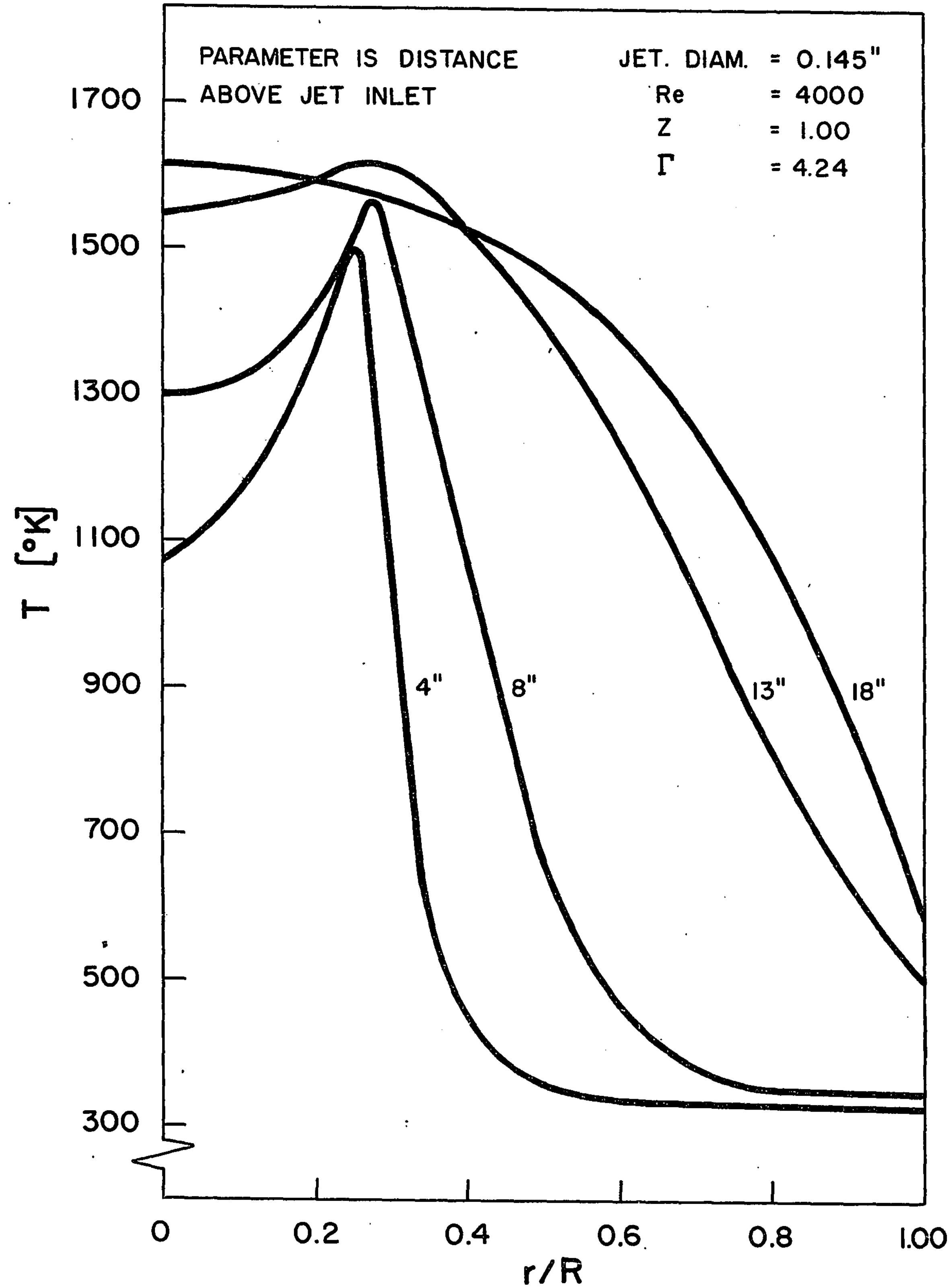

FIGURE 16. TEMPERATURE PROFILES

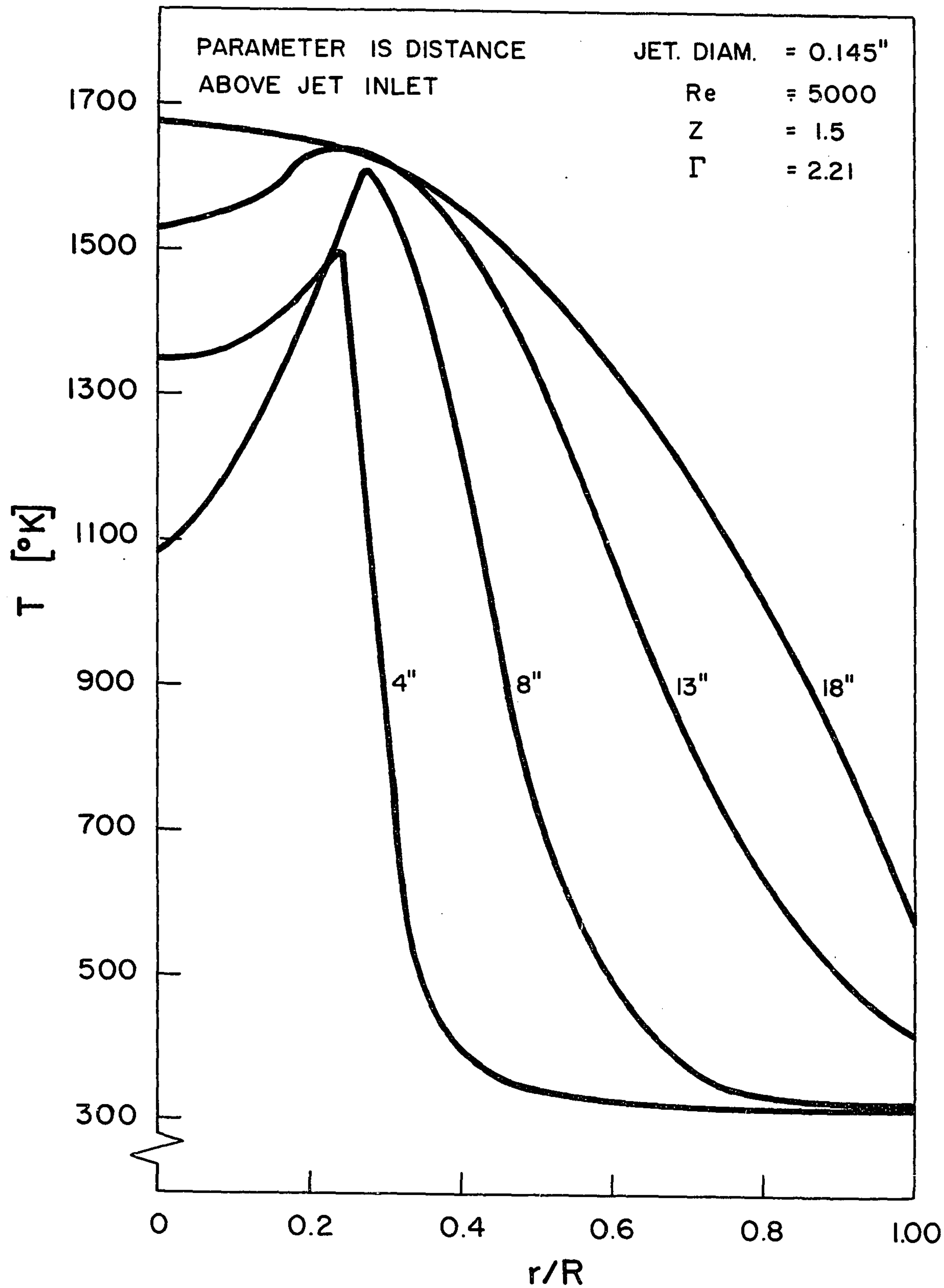

FIGURE 17. TEMPERATURE PROFILES

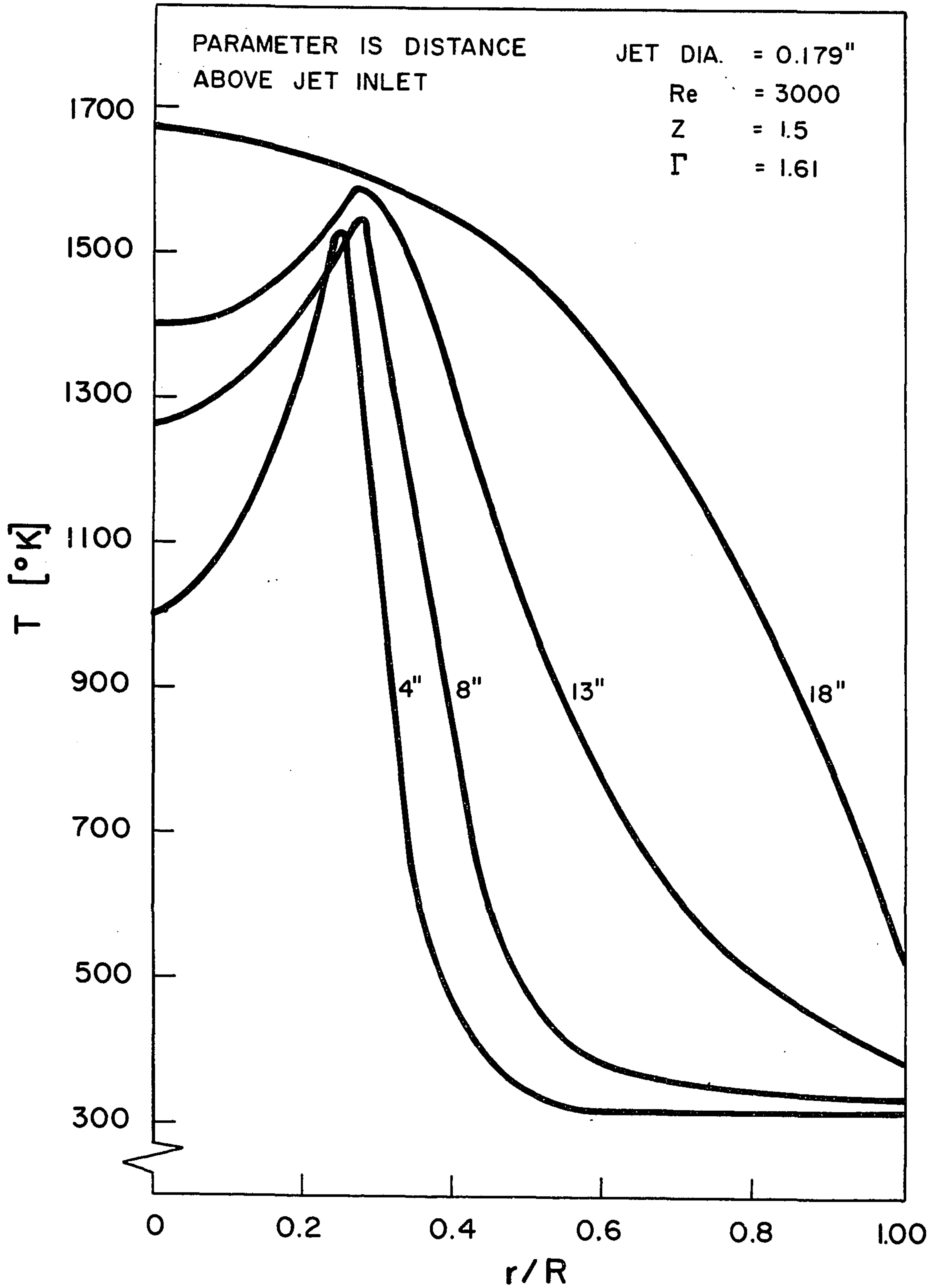

FIGURE 18. TEMPERATURE PROFILES

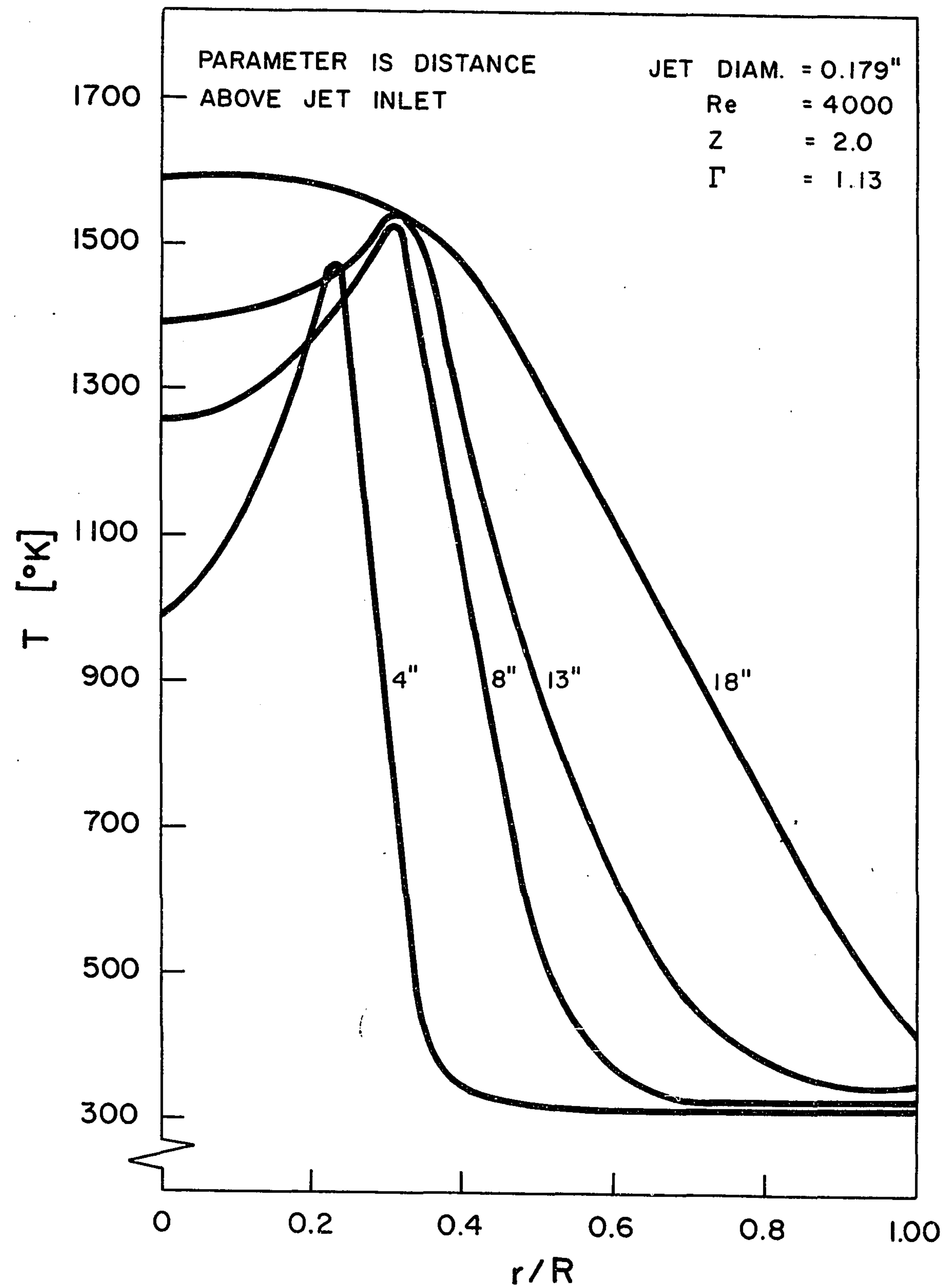

FIGURE 19. TEMPERATURE PROFILES

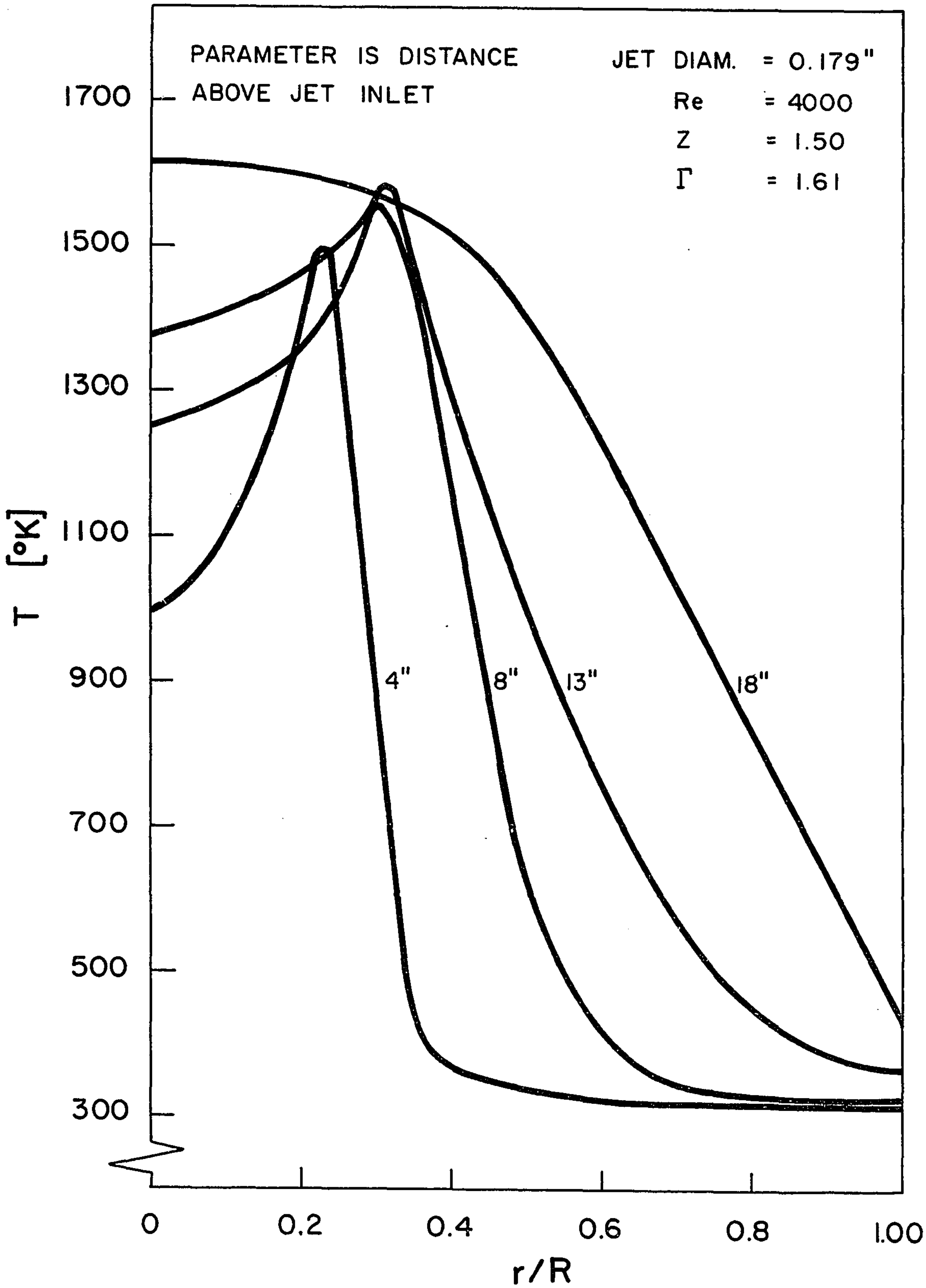

FIGURE 20. TEMPERATURE PROFILES

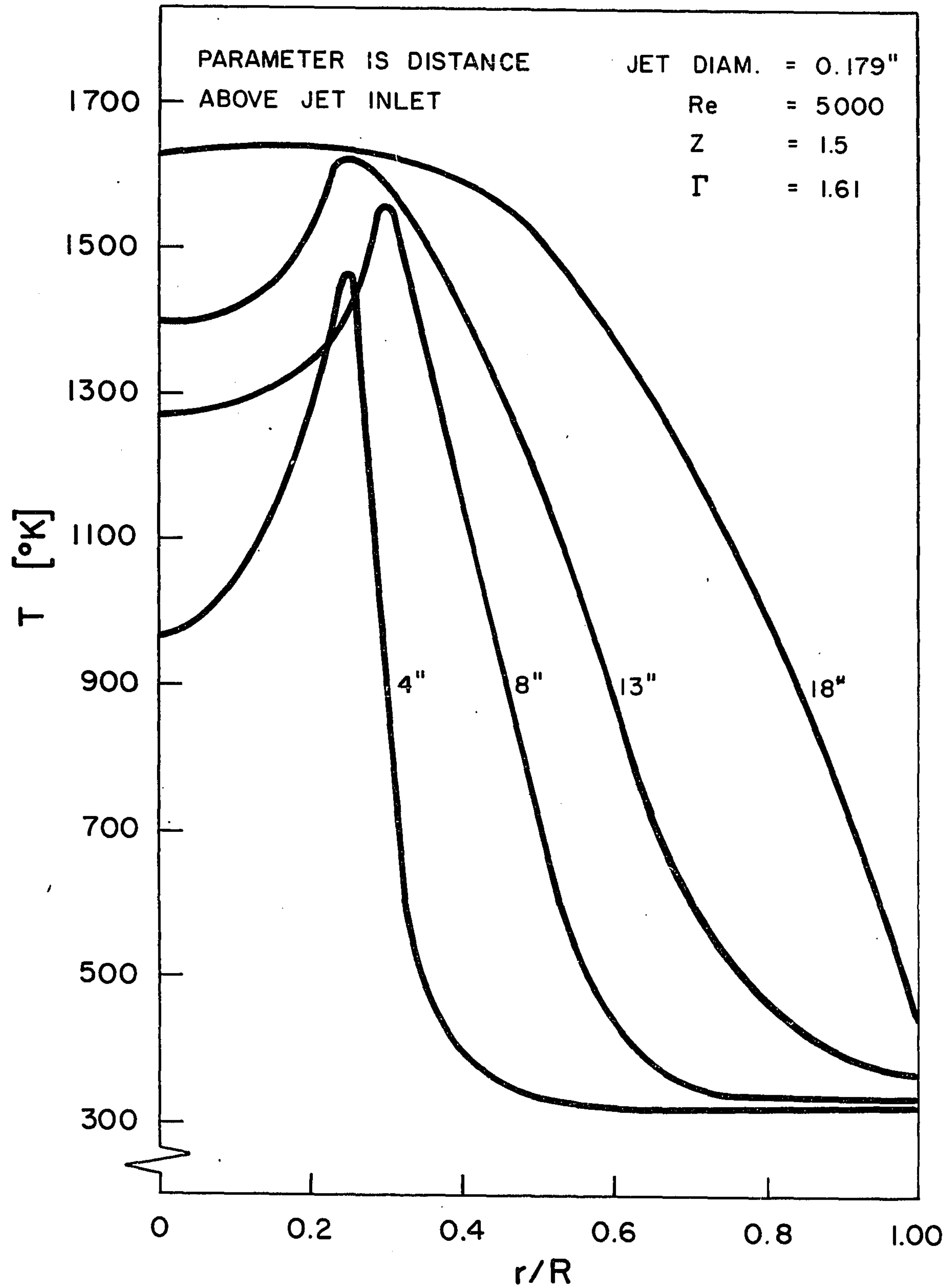

FIGURE 21. TEMPERATURE PROFILES

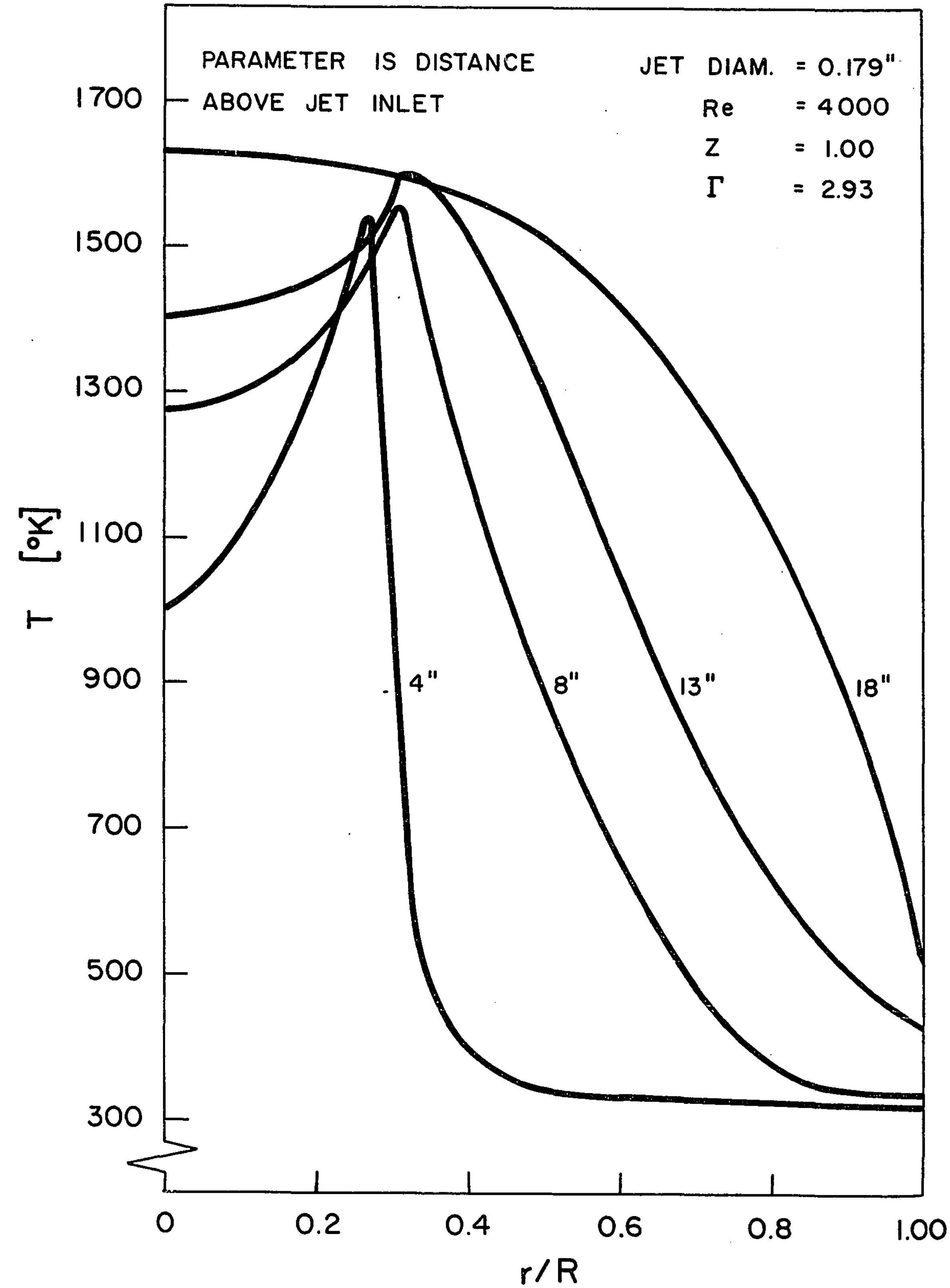

FIGURE 22. TEMPERATURE PROFILES

DIMENSIONLESS WA

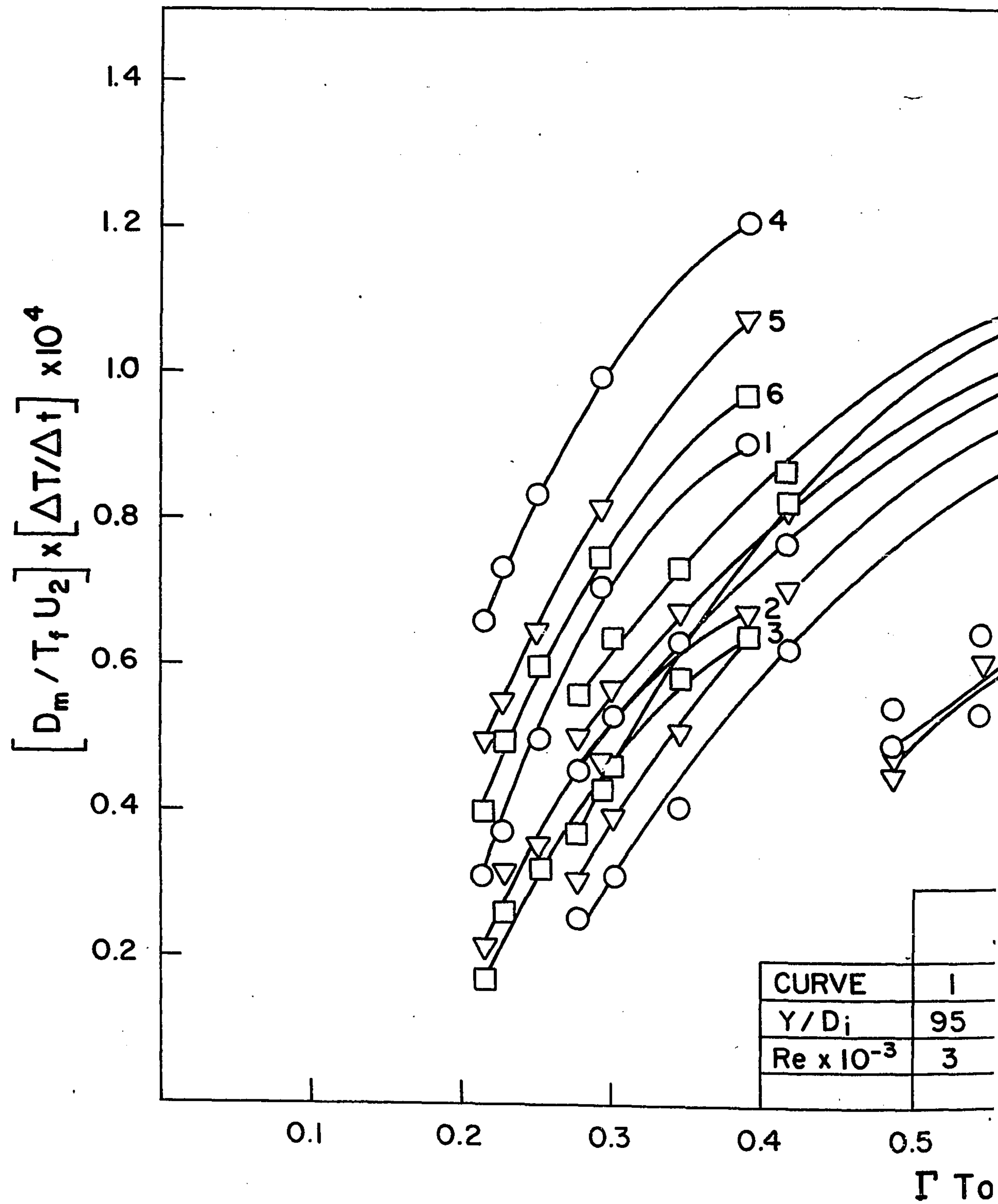

FIGURE 23.

ESS WALL HEATING RATE

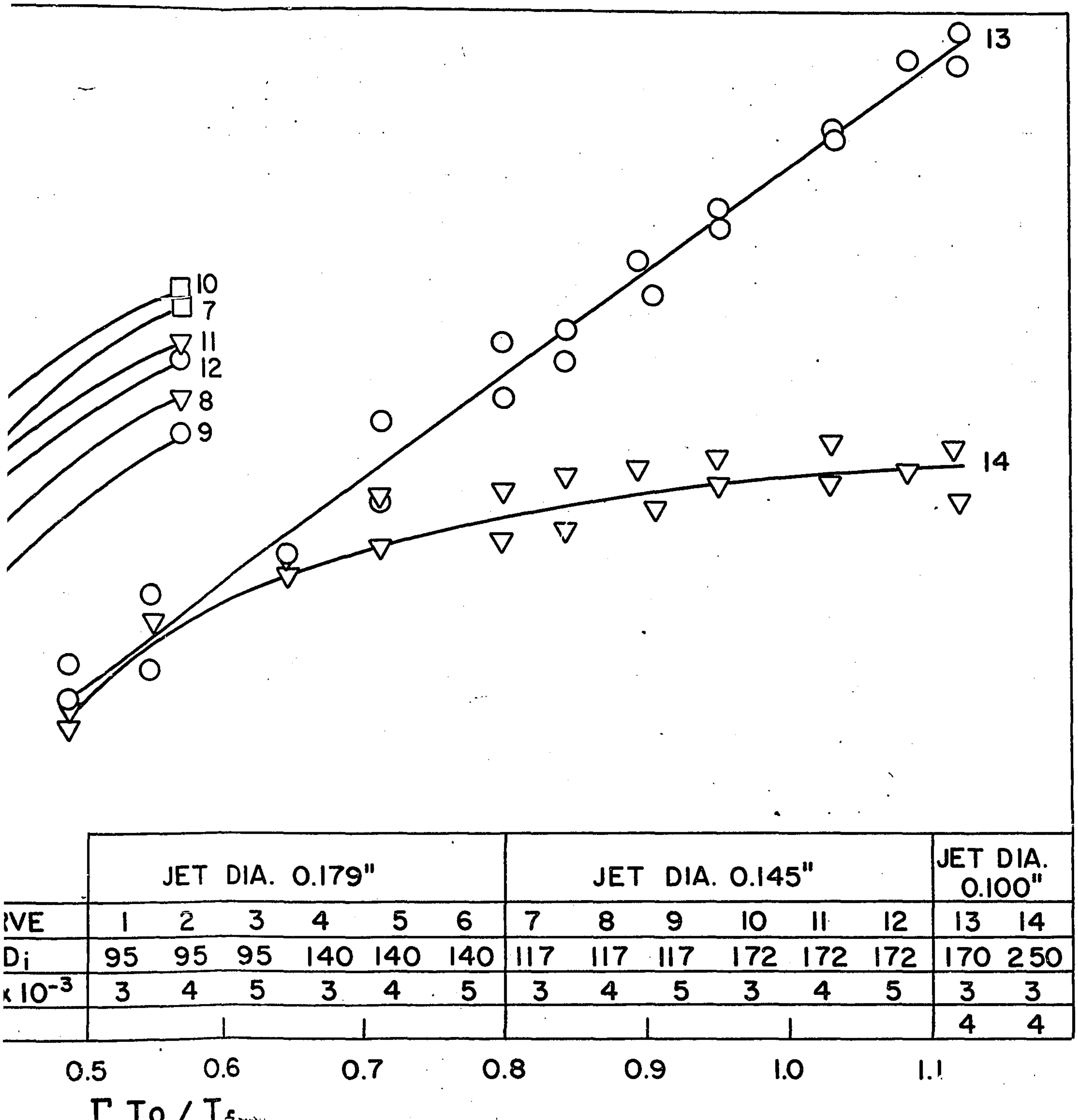

	JET DIA. 0.179"						JET DIA. 0.145"						JET DIA. 0.100"	
RVE	1	2	3	4	5	6	7	8	9	10	11	12	13	14
Di	95	95	95	140	140	140	117	117	117	172	172	172	170	250
x 10^{-3}	3	4	5	3	4	5	3	4	5	3	4	5	3	3
													4	4

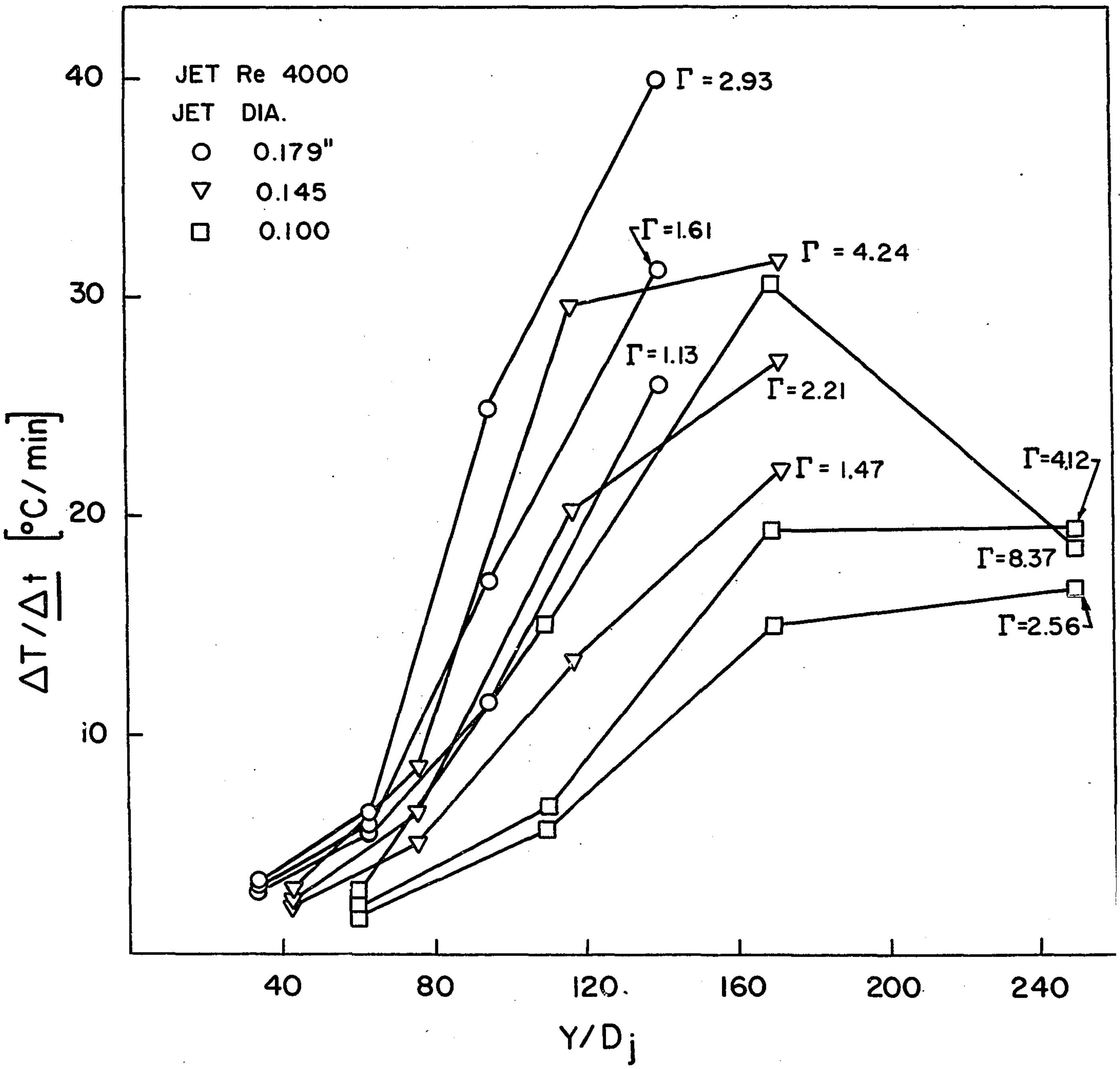

FIGURE 24. VERTICAL VARIATION OF WALL HEATING RATE

V

DISCUSSION OF RESULTS

A. Temperature Profiles

In each of figures 9 - 22, four temperature profiles, measured at different distances above the jet inlet, are presented to show the influence of the jet diameter, jet velocity, air equivalent ratio and the distances above the jet source on temperature profiles inside the furnace. For all three jets, the temperature profiles measured 4" and 8" above the jet source had a maximum at the jet boundary where the chemical reaction is occurring. These maximum temperatures were approximately 500° C lower than the corresponding adiabatic methane flame temperatures for an air equivalent ratio 1. This is in agreement with the results of S.R. Smith and A.S. Gordon for the air-methane diffusion flame (20). The same profiles had a minimum in temperature at the axis which indicated the expected presence of unburned methane gas inside the jet. The minimum at the axis was no longer present in the temperature profiles measured 13" above the jet inlet for the 0.100" jet, or in profiles measured 18" above the jet source for all jets. This same phenomenon was observed at all jet velocities. This confirms the general rule that the length of a turbulent diffusion flame is a function of the jet diameter but is nearly independent of jet velocity.

Recirculation of the hot flue gases outside the jet would tend to increase the temperature closer to the wall of the furnace and to flatten the temperature profile. This tendency can definitely be observed in the measured temperature profiles at different flow conditions, for high values of Γ, where recirculation was expected. However, the mixing of the recirculating hot flue gases with the cold upcoming air would tend to diminish this effect, especially since no chemical reaction can occur between air and combustion products. The temperatures in the reaction zone were substantially higher than those outside the flame in all cases and this made it very difficult to distinguish between non-recirculating flows, and those with slight recirculation, on the basis of temperature profiles.

B. Wall Temperatures

Wall heating rates at several distances above the jet inlet, for different flow conditions, are presented in figures 23 and 24. The heat transferred from the flame to the wall of the furnace results from a combination of radiation and convection, and is a complex function of the temperature distribution, flow conditions and the properties of the fluid. The presence of some degree of similarity in the temperature profiles measured, and the approximate uniformity of maximum temperature from one experiment to another suggest that radiation flux was approximately constant in all experiments, and that the changes in the heating rates of the wall were primarily due to the changes in convective heat flux, which depended to a greater extent on flow regime than did radiation.

In order to deduce something about flow regime, the measured wall heating rates, as indicated by the thermocouples located 17" and 25" above the jet inlet, were plotted in dimensionless form versus $(\Gamma T_o/T_f)$ for all jet sizes, various jet tube Reynolds numbers and various air equivalent ratios. This procedure permitted the presentation on one plot of data for the fairly large range of fuel flow rates studied and the different jets used and resulted in a well behaved family of smooth curves for all the data up to a value of $(\Gamma T_o/T_f)$ of approximately 0.6. For higher values of $(\Gamma T_o/T_f)$ a change in the general shape of the curves can be observed, which suggests that a change in flow regime occurs and that the curves tend to diverge above this critical value. However, it is difficult to draw any more specific conclusions or to estimate the critical value of $(\Gamma T_o/T_f)$ exactly. The value of 0.6 ± 0.1 was estimated as the critical value of $(\Gamma T_o/T_f)$.

The tendency toward increasing heating rates for shorter distances above the jet source due to the recirculating hot flue gases can also be observed in figure 24.

The dimensionless heating rate ($\Delta T/\Delta t$) has been plotted versus dimensionless distance (y/D_j) above the jet inlet for different flow conditions as denoted by the value of Γ. This figure demonstrates in a simple manner the effect of flow regime on wall temperature distributions.

VI

CONCLUSIONS AND RECOMMENDATIONS

A confined turbulent diffusion flame has been studied by measuring the temperature profiles and wall temperatures for different flow conditions. An attempt has been made to develop a criterion for the onset of recirculation in such a system from the furnace design data only.

The cold model, which has proved to be useful in predicting certain flow characteristics in incompressible flow studies of similar geometry, served as a guide for the present approach. However, the complexity of the problem is vastly increased when the incompressible jet is replaced by a diffusion flame. A number of very rough approximations had therefore to be made to derive a mathematical expression for the critical condition for the onset of recirculation. This condition was expressed in terms of a dimensionless parameter called Γ, which is a function only of boundary conditions of the system.

An experimental method was developed and tested to measure temperature profiles inside the furnace, with estimated accuracy better than 4%.

Observed wall temperature distributions were correlated with the values of $(\Gamma T_o/T_f)$. Because of complex interplays between heat release and heat transfer in such a system, it was especially difficult to detect the precise transition between recirculating and non-recirculating flow from temperature measurement only. However, an approximate critical value of the dimensionless group ($\Gamma T_o/T_f$) was obtained, which can be used to predict the onset of recirculation solely from furnace design data.

With the use of a blower for the air, pressure fluctuations introduced by blower itself far exceeded the average static wall pressure differences along the test section, and no reliable pressure measurements could be obtained. The particle track method, a commonly used flame visualization technique, is experimentally difficult and no useful results were obtained using this method.

More experiments are needed in order to confirm and to generalize the present results. A more sensitive experimental method should be developed for indicating the existence of recirculation.

Chemical analysis and point sampling are needed for more detailed study of the system. Point sampling and analysis inside the flame are experimentally very difficult, but sampling outside the flame could give some interesting information as to existence of recirculation. The presence and the concentration of reaction products due to recirculation in the region closer to the jet source might be a sensitive indicator. To determine the completeness of combustion, an analysis of flue gases would be useful.

APPENDIX

Tabulation of Experimental Wall Temperatures measured at various distances above the jet inlet.

Experimental Wall Temperatures measured at various distances above the jet inlet

Jet Diameter 0.179"

Re	Air eqv. Ratio z	$(\Delta T/\Delta t)_{25''}$ ($^oC/min$)	$(\Delta T/\Delta t)_{17''}$ ($^oC/min$)	$(\Delta T/\Delta t)_{11''}$ ($^oC/min$)	$(\Delta T/\Delta t)_{6''}$ ($^oC/min$)	$\Gamma T_o/T_f$	U_2/U_1
3000	2.00	26.2	12.4	4.6	2.3	0.216	0.040
3000	1.75	28.4	14.4	5.2	2.3	0.227	0.035
3000	1.50	30.3	18.2	5.6	2.4	0.252	0.030
3000	1.25	33.2	23.8	6.5	2.7	0.295	0.025
3000	1.00	34.0	28.5	7.5	2.9	0.393	0.020
4000	2.00	26.1	11.4	5.5	2.8	0.216	0.040
4000	1.75	28.4	16.6	5.6	2.9	0.227	0.035
4000	1.50	31.3	17.0	5.7	2.9	0.252	0.030
4000	1.25	36.2	20.8	5.9	2.9	0.295	0.025
4000	1.00	40.4	25.4	6.5	3.1	0.393	0.020
5000	2.00	26.5	11.2	5.1	3.6	0.216	0.040
5000	1.75	32.1	17.1	6.1	3.8	0.227	0.035
5000	1.50	36.6	19.4	7.4	4.0	0.252	0.030
5000	1.25	41.5	23.9	9.6	4.2	0.295	0.025
5000	1.00	45.8	30.3	10.8	4.3	0.393	0.020

Experimental Wall Temperatures measured at various distances above the jet inlet

Jet Diameter 0.145"

Re	Air eqv. Ratio z	$(\Delta T/\Delta t)_{25''}$ (°C/min)	$(\Delta T/\Delta t)_{17''}$ (°C/min)	$(\Delta T/\Delta t)_{11''}$ (°C/min)	$(\Delta T/\Delta t)_{6''}$ (°C/min)	$\Gamma\ T_o/T_f$	U_2/U_1
3000	2.00	18.7	12.2	4.3	2.1	0.280	0.026
3000	1.75	20.5	15.9	5.3	2.2	0.302	0.023
3000	1.50	22.1	17.7	5.9	2.4	0.346	0.020
3000	1.25	24.0	22.8	7.4	2.6	0.418	0.016
3000	1.00	25.8	25.4	9.1	2.9	0.568	0.013
4000	2.00	22.1	13.4	5.0	2.1	0.280	0.026
4000	1.75	24.5	17.1	5.7	2.3	0.302	0.023
4000	1.50	27.2	20.3	6.4	2.5	0.346	0.020
4000	1.25	30.0	26.3	7.1	2.7	0.418	0.016
4000	1.00	31.8	29.6	8.4	2.9	0.568	0.013
5000	2.00	25.3	14.1	5.5	2.6	0.280	0.026
5000	1.75	28.6	16.8	5.9	2.8	0.302	0.023
5000	1.50	31.8	20.2	6.8	2.9	0.346	0.020
5000	1.25	35.5	28.7	8.2	3.1	0.418	0.016
5000	1.00	38.8	34.7	9.9	3.3	0.568	0.013

Experimental Wall Temperatures measured at various distances above the jet inlet

Jet Diameter 0.100"

Re	Air eqv. Ratio z	$(\Delta T/\Delta t)_{25''}$ ($^{\circ}$C/min)	$(\Delta T/\Delta t)_{17''}$ ($^{\circ}$C/min)	$(\Delta T/\Delta t)_{11''}$ ($^{\circ}$C/min)	$(\Delta T/\Delta t)_{6''}$ ($^{\circ}$C/min)	$\Gamma T_o/T_f$	U_2/U_1
3000	2.00	13.3	12.5	4.9	1.4	0.488	0.012
3000	1.75	13.7	14.4	5.5	1.6	0.546	0.011
3000	1.50	14.1	14.8	7.8	1.7	0.646	0.0094
3000	1.375	14.4	18.0	8.7	1.9	0.713	0.0086
3000	1.25	14.0	19.4	9.6	2.0	0.801	0.0078
3000	1.20	13.9	18.5	10.2	2.0	0.844	0.0075
3000	1.14	14.0	19.7	12.2	2.2	0.906	0.0071
3000	1.10	14.3	21.1	11.8	2.3	0.953	0.0069
3000	1.05	13.9	22.4	12.7	2.4	1.032	0.0066
3000	1.00	12.8	24.1	13.0	2.6	1.122	0.0063
4000	2.00	16.8	15.2	5.6	1.9	0.488	0.012
4000	1.75	18.5	15.8	6.9	2.2	0.546	0.011
4000	1.50	19.6	19.4	8.3	2.4	0.646	0.0094
4000	1.375	20.8	20.8	9.2	2.4	0.713	0.0086
4000	1.25	20.4	23.8	10.5	2.5	0.801	0.0078
4000	1.20	20.5	25.9	11.2	2.6	0.844	0.0075
4000	1.15	20.3	27.7	11.9	2.7	0.895	0.0072
4000	1.10	20.1	28.6	12.9	2.7	0.953	0.0069
4000	1.05	19.7	30.0	14.0	2.8	1.032	0.0066
4000	1.00	18.7	30.8	15.0	3.0	1.122	0.0063

REFERENCES

1. Abramovich, G., The Theory of Turbulent Jets, M.I.T. Press, 1963.

2. Alvermann, W., and Stottmann, P., "Temperature measurements in combustion gases by means of thermocouples" (in German), Deutsche Luft - und Raumfahrt Forschungbe 64 - 18, 38, (July 1964).

3. Becker, H.A., Concentration Fluctuations in Ducted Jet-mixing, Sc. D. Thesis, Chem. Eng., M.I.T., 1961.

4. Becker, H.A., Hottel, H.C., and Williams, G.C., "Mixing and Flow in Ducted Turbulent Jets", Ninth Symposium on Combustion 1962, 7, Academic Press, (1963).

5. Bone, W.A. and Townend, D.T.A., Flame and Combustion in Gases, Longmans, Green and Co., Inc., New York, (1927).

6. Cooper, R.G., Velocity Profiles and Pumping Capacities of Turbine Type Impellers, M.Eng. Thesis, Chem. Eng., McGill University, (1966).

7. Curtet, R., "Sur l'Ecoulement d'un Jet Entre Parois", Publ. Scientifiques et Techniques du Ministere de l'Air, No. 359, (1960).

8. Dealy, J.M., Momentum Exchange in a Confined Circular Jet with Turbulent Source, Ph.D. Thesis, University of Michigan, (1963).

9. Dealy, J.M., "The Confined Circular Jet With Turbulent Source", Symp. on Fully Separated Flows, p. 84, (May 1964).

10. Fristrom, R.M., and Westenberg, A.A., Flame Structure, McGraw-Hill Book Co., New York, (1965).

11. Hedley, A.B. and Jackson, E.W., "Recirculation and its effects in Combustion Systems", J. Inst. Fuel, 38, 290, (July 1965).

12. Hedley, A.B., and Jackson, E.W., "The Effect of Recirculation on Reaction Rates in a Homogeneous Combustion System", Trans. Inst. Chem. Engrs. 44, 3, T 85 - T 90, (1966).

13. Hinze, J.O., Turbulence, McGraw-Hill Book Co., Inc., New York, (1959).

14. Hirschfelder, J.O., Curtiss, C.F., and Bird, R.B., Molecular Theory of Gases and Liquids, John Wiley and Sons, Inc., New York, (1954).

15. Hottel, H.C., and Sarofim, A.F., "The Effect of Gas Flow Patterns on Radiative Transfer in Cylindrical Furnaces", Int. J. of Heat and Mass Transfer, 8, 1153, (1965).

16. Kaskan, W.E., "The Dependence of Flame Temperature on Mass Burning Velocity", Sixth Symp. on Combustion 134, Reinhold Publishing Corporation, New York, (1957).

17. Lewis, B., and von Elbe, G., Combustion, Flames and Explosions of Gases, Academic Press, New York, (1961).

18. McAdams, W.H., Heat Transmission, Ed. 3, 259, McGraw-Hill Book Co., New York, (1954).

19. Schlichting, H., Boundary Layer Theory, Pergamon Press, London, (1958).

20. Smith, S.R., and Gordon, A.S. "The Methane Diffusion Flame", J. Phys. Chem., 60, 759, (1956).

21. Steffensen, R.J., Agnew, J.T., and Olsen, R.A., "Combustion of Hydrocarbons - Property Tables", Engineering Bulletin of Purdue University No. 122, Purdue U., Lafayette, Indiana, (May 1966).

22. Summerfield, M., Reiter, S.H., Kebeley, V., and Mascolo, R.W., "The Structure and Propagation Mechanism of Turbulent Flames in High Speed Flow", Jet Propulsion, 25, 377, (1955).

23. The NBS-NACA "Tables of Properties of Gases", National Bureau of Standards, Washington, (1950).

24. Thring, M.W., and Newby, M.P., "Combustion Length of Enclosed Turbulent Jet Flames", Fourth Symp. on Combustion, 789, The Williams and Wilkins Co., Baltimore, (1953).

25. Townsend, A.A., The Structure of Turbulent Shear Flow, Cambridge University Press, Cambridge, (1956).

NOMENCLATURE

Some symbols defined in the text and used only once are not listed here.

Symbol	Meaning
D	diameter
D_j	diameter of jet source
D_m	diameter of mixing tube
K	constant (defined in equation (II.13))
M	mass flux
m	Curtet similarity parameter
m_o	initial value of m (defined in equation (I.1))
Q	volumetric flow rate
Q_t	total flow rate in mixing tube
P	pressure
R_1	radius of jet source
R_2	radius of mixing tube
r	radial coordinate
T	temperature
T_f	adiabatic flame temperature
T_o	room temperature
t	time
u	velocity in axial direction
$\bar{u}$	average velocity over cross section
U_1	jet source velocity

Symbol	Meaning
U_2	secondary flow velocity at y=0
y	axial coordinate, measured from source
z	air equivalent ratio
Ct	Craya-Curtet number (defined in equation (I.2))
M	Mach number
Re	jet source Reynolds number
α	heat transfer coefficient
β_1	momentum factor for turbulent pipe flow
β_ρ	generalized momentum factor (defined in equation (II.9))
Γ	momentum parameter (defined in equation (II.10))
Δ	difference, finite
ϵ	emissivity
λ	heat conductivity
μ	viscosity
ρ	density
$\bar{\rho}$	average density over cross section
ρ_1	fuel density
ρ_2	air density

Subscripts:

1	jet flow
2	secondary flow

Subscripts Cont'd.	Meaning
o	value at $y=0$
r	value at $y=y_r$
rad	radiation
w	wire